NATIONAL AERONAUTICS AND SPACE ADMINISTRATION
CONTRACT NO. NAS 7-100

Technical Report No. 32-223

Space Trajectories Program for the IBM 7090 Computer

D. B. Holdridge

W. R. Hoover

W. R. Hoover, *Chief*
Computer Applications and Data Systems

JET PROPULSION LABORATORY
CALIFORNIA INSTITUTE OF TECHNOLOGY
PASADENA, CALIFORNIA
March 2, 1962

CONTENTS

TABLES

ABSTRACT

The Space Trajectories Program for the IBM 7090 computer is described in comprehensive detail, with emphasis on the development of the equations. Equations of motion for both the Cowell and Encke methods are given. Numerical experience with the class of trajectories encountered in practice is included to compare the Cowell and Encke methods, and to obtain an estimate of the over-all accuracy of the program. Sources of error are pointed out, consistent with the precision of the numerical methods. Operating instructions and descriptions of input and output are provided for the successful running of trajectories. Flow charts presented serve as a guide to the understanding of the internal sequence of events and control methods. Major subroutines used in the program are contained in the Appendix. The program is written in the FORTRAN Assembly Program language.

I. INTRODUCTION

The Space Trajectories Program originated in the need to study trajectories of high precision formed by the transit of a space probe from the Earth to one of the three targets technologically feasible at present — the Moon, Venus, or Mars — under the influence of gravitational forces described by Newton's law alone. Although the major programming effort has gone into obtaining a solution for which the accuracy is consistent with the single-precision arithmetic used, and which requires a reasonable amount of computer time (about 30 seconds), the program may be used for study of general interplanetary flight where it is sufficient to include the bodies Sun, Venus, Earth, Moon, Mars, and Jupiter for their gravitational influence.

Since the program solves the equations of motion for the probe only, and ignores the negligible perturbations of the probe on the bodies, it is sufficient to obtain the positions and velocities of the bodies in the form of planetary and lunar ephemerides in some convenient reference frame. Since the coordinates have been traditionally referred to the Cartesian system based on the mean equator and equinox of 1950.0, the ephemerides used by the program have been uniformly expressed in the same coordinate system. The collection of ephemerides was systematically done on magnetic tape.[1]

Having expressed the coordinates of the bodies in the 1950.0 reference, it was natural to write the equations of motion in the same coordinate system. But it was immediately necessary to obtain expressions for the precession

[1]A description of the standard source tape with origins is given in "Subtabulated Lunar and Planetary Ephemerides," by R. H. Hudson, Technical Release No. 34-239, Jet Propulsion Laboratory, Pasadena, Calif., November 2, 1960.

and nutation of the Earth's equator so that the oblateness perturbation of the Earth might be properly assessed in the 1950.0 frame and that injection conditions referenced to the Earth's true equator of date resulting from powered-flight arcs might be rotated to the fixed system. To assist in the latter transformation, the hour angle at Greenwich of the true vernal equinox was obtained by the synthesis of a calculated mean value and the nutation in right ascension formed from the nutations and the obliquity of the ecliptic.

As the planetary-position ephemerides are tabulated at four-day intervals and the lunar at one-day intervals on the ephemeris tape, it was necessary to use an interpolation scheme to obtain intermediate values of positions and velocities. An Everett's formula which utilizes second and fourth central differences was chosen for the positions; to obtain the velocities, the Everett's interpolating polynomials were differentiated to obtain polynomials to be applied to the tabulated positions. It was found convenient to tabulate the necessary differences on the ephemeris tape along with the positions, and to arrange the tape in 20-day records to permit efficient tape scanning in either the forward or the backward direction, and to avoid excessive tape reference; thus lunar trajectories require, at most, two records, and interplanetary on the order of ten, which keeps tape-handling time within reasonable limits. Additionally, for the Moon, the sixth and eighth central differences have been thrown back on the second and fourth, since the former are not negligible. To handle long flight times, the argument is carried in double precision; this technique also allows for smooth interpolation.

The equations of motion have been written to take advantage of the fact that usually a central body may be found, and the coordinates relative to that body expressed so that the dominant term in the acceleration arises from the chosen body, and the remaining terms are relatively small perturbations acting to displace the two-body orbit formed by the trajectory of the probe in the field of the central body alone. Thus the remaining gravitational bodies give rise to what is known as the n-body perturbation; the perturbation arising from the oblateness of the Earth and expressed by the second, third, and fourth harmonics is included when the probe is near the Earth; in a similar manner, the perturbation derived from the triaxial figure of the Moon and represented through a second harmonic term is included when the probe is in the vicinity of the Moon. The above method of representing the equations of motion is known as a Cowell scheme. If the central-body term is replaced by the acceleration arising from the deviation of a true orbit from a fixed reference two-body orbit and the equations of motion are referred to the deviation, then the method is called an Encke scheme. Either the Cowell or the Encke scheme may be used in the program, although the latter is generally preferred in practice because of a small advantage in speed and accuracy. But for the powered flight option, which simulates the burning of a constant-thrust motor, a Cowell scheme is generally advisable because the rapid deviation from the reference two-body orbit would force frequent recalculation of the reference if the Encke scheme were used. The motor is assumed to be of high thrust since the attitude is forced to remain fixed in space, a restriction which is unrealistic for a low-thrust motor.

The solution to the trajectory problem is obtained by a stepwise numerical integration of the equations of motion appropriate to either the Cowell or Encke scheme according to an Adams-Moulton predictor-corrector method which retains the sixth differences of the derivatives; a Runge-Kutta method accurate through fourth order is used to obtain starting values for the Adams-Moulton method. An additional refinement is the fact that the ordinates are accumulated in double precision to control the growth of roundoff error. To obtain the solution at desired points, the subroutine MARK is employed. (For details of subroutines, see Appendix.)

For purposes of control, the trajectory has been divided into segments which are referred to as "phases." Usually a phase is characterized by a dominant central body, and integration step size is determined by the distance of the probe from that body. Thus a normal Venus trajectory which injects near perigee and terminates with Venus impact would consist of three phases: phase one, integration to 2.5×10^6 km from the Earth, with the Earth as the central body; phase two, Sun-centered integration to 2.5×10^6 km from Venus; and phase three, Venus-centered integration to the surface of Venus at 6100 km. In addition, the phase may be used for the auxiliary function of controlling the density, type, and incidence of output.

The program operates internally in laboratory units, i.e., in kilometers and seconds, rather than the classical units utilized in celestial mechanics. Universal Time (U.T.) is used, although provisions have been made to augment U.T. by a constant to obtain Ephemeris Time (E.T.) for use as the argument of the ephemerides. For purposes of high resolution, time is carried in double-precision seconds past 0^h January 1, 1950. This choice also makes for consistent results, even though the phase-transfer points

may be changed somewhat for a particular trajectory; otherwise, the interpolated values of the coordinates might not be a smooth function of time, and hence give rise to systematic errors at the transfer point.

The motion of the Moon's true equator has been accurately represented by the program to provide for selenographic coordinates to be used for both input and output. The rotation necessary to transform from the 1950.0 reference to selenographic Cartesian coordinates is also needed to represent the perturbation arising from the nonspherical figure of the Moon. The description of the selenographic quantities may be found in the discussions of subroutines NUTATE, MNA, MNAMD, and XYZDD[2] given in the Appendix.

In summary, the Space Trajectories Program in its present form is the culmination of three years of work in the space trajectory field at the Jet Propulsion Laboratory, and is designed for the study of the motion of a space probe confined to the solar system and influenced by the nonspherical Earth and Moon, and the point masses defined by the Sun, Venus, Mars, and Jupiter. The program may also be employed in other applications, of which the following are some examples. A simplified powered-flight arc may be simulated which assumes a constant-thrust, constant-burning-rate motor with thrust direction fixed in space. Any of the above-mentioned bodies may serve as the reference body at the injection epoch, and stepwise numerical integration of the equations of motion appropriate to either a Cowell or an Encke scheme serves to step the probe along its flight path to one of the bodies, which then serves as a target. Standard-type trajectories injecting near the Earth, and having as target one of the bodies Earth, Moon, Venus, or Mars, have been given special treatment to reduce the volume of input necessary for execution. The injection conditions may be input in Cartesian or spherical coordinates based on one of four reference frames: mean equator and equinox of 1950.0, mean equinox and ecliptic of 1950.0, true equator and equinox of date, and the true equinox and ecliptic of date. For the Earth as injection body, the Earth-fixed spherical set, based on a rotating Earth, is available; for the Moon as injection body, the selenographic (Moon-fixed spherical) coordinate set, which takes into account the rotation of the Moon, may be used. For injection conditions taken with reference to the Earth, a quasi-orbital element set for escape hyperbolas, known as the energy-asymptote option, has been made available. For output, any of the above quantities may be obtained at will, along with ephemeris information expressed in any one of the four Cartesian or spherical coordinate systems; conic output may be called for which expresses the osculating two-body orbit in many sets of orbital elements referred to one of the standard Cartesian frames; all manner of the principal angles between the probe and the bodies may be displayed; up to a maximum of 15 tracking stations may be used to observe the probe in topocentric spherical coordinates; or view periods of the stations may be determined by the program and displayed in the form of rise, maximum elevation, and set prints.

[2]These subroutines were programmed with minor revisions from the equations described in "Selenographic Coordinates," by B. E. Kalensher, Technical Report No. 32-41, Jet Propulsion Laboratory, Pasadena, Calif., February 24, 1961.

II. EQUATIONS OF MOTION

A. Cowell Scheme

Let there be a small probe, body 0, in the gravitational field of n other bodies. Choosing an inertial frame of reference results, according to Newton, in

$$\ddot{\boldsymbol{\rho}}_i = -k^2 \sum_{\substack{j=0 \\ j\neq i}}^{n} m_j \frac{\boldsymbol{\rho}_{ji}}{\rho_{ji}^3} \qquad i = 0,\ldots,n \qquad (1)$$

where $\boldsymbol{\rho}_{ji} = \boldsymbol{\rho}_i - \boldsymbol{\rho}_j$; $\rho_{ji} = |\boldsymbol{\rho}_{ji}|$; $i, j = 0,\ldots,n$; and k is the gaussian gravitational constant (Sketch 1).

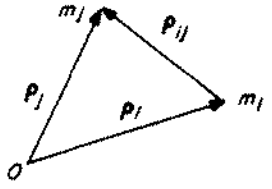

Sketch 1. Relationship of ith and jth body in an inertial frame centered at O

Observe that

$$\mathbf{P} = \frac{1}{M} \sum_{j=0}^{n} m_j \boldsymbol{\rho}_j$$

the center of mass, has the interesting property that

$$\ddot{\mathbf{P}} = \frac{-k^2}{M} \sum_{j=0}^{n} m_j \sum_{\substack{i=0 \\ i\neq j}}^{n} m_i \frac{\boldsymbol{\rho}_{ij}}{\rho_{ij}^3} = \mathbf{0}$$

since

$$\boldsymbol{\rho}_{ij} = -\boldsymbol{\rho}_{ji}$$

and

$$\rho_{ij} = \rho_{ji} \quad \text{with } M = \sum_{j=0}^{n} m_j$$

Therefore $\dot{\mathbf{P}}$ is constant and the barycenter is an inertial frame.

Were it sufficient to express the motion of the probe, body 0, in an inertial coordinate system, the result would be

$$\ddot{\boldsymbol{\rho}}_0 = -k^2 \sum_{j=1}^{n} m_j \frac{\boldsymbol{\rho}_{j0}}{\rho_{j0}^3} \qquad (2)$$

where the coordinates are referred to the barycenter. Such a representation would naturally enough be called the barycentric form of the equations of motion. However, in practice it is convenient to rewrite Eq. (2) so that the coordinate system is referred to one of the n bodies, usually the dominant one.

Using Eq. (2) above with $l \geqq 1$ as the central body

$$\ddot{\mathbf{R}}_0 + \ddot{\boldsymbol{\rho}}_l = -k^2 \sum_{j=1}^{n} m_j \frac{\mathbf{R}_{j0}}{R_{j0}^3}$$

with

$$\mathbf{R}_i = \boldsymbol{\rho}_i - \boldsymbol{\rho}_l = \boldsymbol{\rho}_{li}$$
$$\mathbf{R}_{ij} = \mathbf{R}_j - \mathbf{R}_i = \boldsymbol{\rho}_j - \boldsymbol{\rho}_i = \boldsymbol{\rho}_{ij}, \quad i,j = 0,\ldots,n$$
$$R_{ij} = |\mathbf{R}_{ij}|$$

defined in the new coordinate system.

To obtain $\ddot{\mathbf{R}}_0$ from the above expression, calculate $\ddot{\boldsymbol{\rho}}_l$ with the aid of Eq. (1):

$$\ddot{\boldsymbol{\rho}}_l = -k^2 \sum_{\substack{j=0 \\ j\neq l}}^{n} m_j \frac{\boldsymbol{\rho}_{jl}}{\rho_{jl}^3} = k^2 \sum_{\substack{j=0 \\ j\neq l}}^{n} m_j \frac{\mathbf{R}_j}{R_j^3}$$

So

$$\ddot{\mathbf{R}}_0 = -k^2 (m_l + m_0) \frac{\mathbf{R}_0}{R_0^3} - k^2 \sum_{\substack{j=1 \\ j\neq l}}^{n} \left(m_j \frac{\mathbf{R}_{j0}}{R_{j0}^3} + m_j \frac{\mathbf{R}_j}{R_j^3} \right)$$

In practice, since $m_0/m_l \approx 0$, write in brief

$$\ddot{\mathbf{R}} = -\mu_l \frac{\mathbf{R}}{R^3} - \sum_{\substack{j=1 \\ j\neq l}}^{n} \mu_j \left(\frac{\mathbf{R}_{jp}}{R_{jp}^3} + \frac{\mathbf{R}_j}{R_j^3} \right) \qquad (3)$$

with $\mathbf{R} = \mathbf{R}_0 = \mathbf{R}_p$, $\mathbf{R}_{jp} = \mathbf{R}_{j0}$, p denoting the probe, and $\mu_j = k^2 m_j$; $j = 1,\ldots,n$.

In Eq. (3), the summation on the right will be known as the n-body perturbation which may be resolved into the direct terms, $-\Sigma \mu_j \mathbf{R}_{jp}/R_{jp}^3$, and the indirect terms, $-\Sigma \mu_j \mathbf{R}_j/R_j^3$; the latter sum represents the accelerating effect of the $n-1$ noncentral bodies on the central body and is what distinguishes Eq. (3) from Eq. (2). The effect of the central body has been deliberately isolated because normally it is the dominant term in the expression for the acceleration. In particular, in the case that all perturbations vanish, Eq. (3) may be solved completely for the geometric orbit, a conic. Even when the perturbations are small, the above conic solution may be used to

rewrite the equations of motion as in Encke's method described in Section IIB.

When the probe is in the vicinity of an oblate body, a perturbing term is added to the differential equations which may be described by the corresponding potential function.

For the Earth, use is made of the second, third, and fourth harmonics:

$$U_\oplus = \frac{\mu_\oplus}{R}\left\{\frac{Ja_\oplus^2}{3R^2}(1-3\sin^2\phi)+\frac{Ha_\oplus^3}{5R^3}(3-5\sin^3\phi)\sin\phi + \frac{Da_\oplus^4}{35R^4}(3-30\sin^2\phi+35\sin^4\phi)\right\}$$

where $\mu_\oplus$ is the gravitational coefficient of the Earth, $a_\oplus$ is the equatorial radius of the Earth, and ϕ is the geocentric latitude. The perturbing acceleration is then given by

$$\nabla U_\oplus = \left(\frac{\partial U_\oplus}{\partial X}, \frac{\partial U_\oplus}{\partial Y}, \frac{\partial U_\oplus}{\partial Z}\right)$$

where $\mathbf{R} = (X, Y, Z)$ and the coordinate system is oriented in the fixed 1950.0 system described in Section IVB. The precise form of $\nabla U_\oplus$ is given in the subroutine HARMN described in the Appendix.

The Moon may be regarded as a triaxial ellipsoid with the explicit expansion for the oblate potential being

$$U_\leftmoon = G\left(\frac{A+B+C-3I}{2R^3}\right)$$

where

$$G = \frac{\mu_\leftmoon}{m_\leftmoon} = k^2$$

$$I = A\left(\frac{x}{R}\right)^2 + B\left(\frac{y}{R}\right)^2 + C\left(\frac{z}{R}\right)^2$$

A, B, and C are moments of inertia about the three principal axes of the ellipsoid and $\mathbf{R} = (x, y, z)$ is the position of the probe expressed in the orthogonal right-handed coordinate system defined by the aforementioned principal axes. Specifically, the $x-y$ plane defines the Moon's true equator, the x axis emanates from the longest axis which is constrained to point in the general direction of the Earth, while the z axis lies in the direction of the Moon's spin vector; the figure may be likened to a distorted oblate spheroid, disfigured because of the Earth's proximity.

To obtain the acceleration, again form $\nabla U_\leftmoon$, with X, Y, Z given in the 1950.0 system. The explicit form of $\nabla U_\leftmoon$ may be found in subroutine XYZDD described in the Appendix; the body-fixed coordinate system for the Moon is given in the discussions of subroutines XYZDD, MNA, and MNAMD in the Appendix.

At times it may be necessary to simulate the performance of a small midcourse motor which burns with constant thrust with an attitude fixed in the 1950.0 reference system. Thrust duration is handled as a function of time alone:

$$\mathbf{a} = -\frac{F}{m_0 - \dot{m}(T-T_0)}\mathbf{C} \qquad T_0 \leqq T \leqq T_1 \qquad (4)$$

where $\mathbf{C}$ is the spin-axis vector of the probe fixed in space, F is the constant thrust, $\dot{m}$ is the constant mass flow rate, and m_0 is the initial mass.

During burning, Eq. (4) represents the largest contribution to the acceleration and Encke's method is not used. In general

$$\ddot{\mathbf{R}} = -\mu\frac{\mathbf{R}}{R^3} + \mathbf{P} \qquad (5)$$

where $\mu = \mu_i$ and $\mathbf{P}$ represents the contributions to the acceleration arising from the above-mentioned perturbations and any thrust which may be considered. The direct numerical integration of Eq. (5) is here defined as a Cowell integration, although the latter term is used differently by other authors.

B. Encke's Method

Let the probe be near a central body so that $\mathbf{P}$ becomes small compared to the central body term in Eq. (5). At the epoch T_0 the two-body problem may be solved with suitable initial conditions. The defining equations of motion for the unperturbed orbit are

$$\ddot{\mathbf{R}}_0 = -\mu\frac{\mathbf{R}_0}{R_0^3} \qquad (6)$$

Thus, $\mathbf{R}_0$ is available and, if necessary, $\dot{\mathbf{R}}_0 = \mathbf{V}_0$ as a function of time. Next, consider the differential equations for $\boldsymbol{\rho} = \mathbf{R} - \mathbf{R}_0$, the Encke displacement, where $\mathbf{R}$ is from the perturbed orbit defined in Eq. (5):

$$\ddot{\boldsymbol{\rho}} = -\mu\left(\frac{\mathbf{R}}{R^3} - \frac{\mathbf{R}_0}{R_0^3}\right) + \mathbf{P} \qquad (7)$$

At this point, the difference between the central-body terms must be expanded by means of the small parameter Q; otherwise, numerical differencing will result in significant errors introduced in the accelerations. So

$$\frac{\mathbf{R}}{R^3} - \frac{\mathbf{R}_0}{R_0^3} = \frac{1}{R_0^3}\left\{\left(\frac{R_0^3}{R^3} - 1\right)\mathbf{R} + \boldsymbol{\rho}\right\} \tag{8}$$

Define, as with Encke, Q by the relation $1 + 2Q = R^2/R_0^2$; in general, when the method is applicable, Q will be a small parameter. Now

$$1 - \frac{R_0^3}{R^3} = 1 - (1 + 2Q)^{-3/2}$$

and the difference may be expanded into the series

$$F(Q) = 1 - (1 + 2Q)^{-3/2} = Q\sum_{j=0}^{m} a_j Q^j \tag{9}$$

where m is chosen so that the remainder in the sum stays smaller than $a_0 \times 10^{-8}$ whenever $|Q| \leqq Q_0$.

An accurate numerical value for Q must be obtained in order to justify the expense of the series expansion in Eq. (9):

$$\begin{aligned} Q &= \frac{1}{2}\left(\frac{R^2}{R_0^2} - 1\right) \\ &= \frac{1}{2}\,\frac{(\mathbf{R}_0 + \boldsymbol{\rho})\cdot(\mathbf{R}_0 + \boldsymbol{\rho}) - R_0^2}{R_0^2} \\ &= \frac{1}{2}\,\frac{R_0^2 + 2\boldsymbol{\rho}\cdot\mathbf{R}_0 + \boldsymbol{\rho}\cdot\boldsymbol{\rho} - R_0^2}{R_0^2} \end{aligned}$$

$$Q = \frac{\boldsymbol{\rho}\cdot\left(\mathbf{R}_0 + \frac{\boldsymbol{\rho}}{2}\right)}{R_0^2} \tag{10}$$

It has been found that the above dot product is well defined numerically for most cases; further numerical safeguards which have been added to control the accuracy of Q are given in subroutine ENCKE, described in the Appendix.

If the difference appearing in Eq. (7) is evaluated, using Eq. (8) and Eq. (9), the final equations of motion for the Encke method become

$$\ddot{\boldsymbol{\rho}} = -\frac{\mu}{R_0^3}(\boldsymbol{\rho} - \mathbf{R}F(Q)) + \mathbf{P} \tag{11}$$

To start the integration at the epoch T_0, an arbitrary set of elements is chosen to describe the two-body motion; in all instances, judicious selection must be made so that the Encke term in Eq. (11) does not become large rapidly and so destroy the advantage over the Cowell method, which uses Eq. (5). In most cases the elements will be osculating, so that $\boldsymbol{\rho}(T_0) \approx 0$ and $\dot{\boldsymbol{\rho}}(T_0) \approx 0$ to the limitations of the numerical calculation. For the Encke initial conditions at the epoch T_0, use

$$\begin{aligned} \boldsymbol{\rho}(T_0) &= \mathbf{R}(T_0) - \mathbf{R}_0(T_0) \\ \dot{\boldsymbol{\rho}}(T_0) &= \dot{\mathbf{R}}(T_0) - \dot{\mathbf{R}}_0(T_0) \end{aligned}$$

If the perturbation $\mathbf{P}$ is large enough, both Q and ρ/R_0 will grow with time; Q may be small while ρ/R_0 is relatively large, since Q is defined by the dot product in Eq. (10). Under these circumstances it becomes necessary to rectify the reference orbit and restart the numerical integration. ρ/R_0 is used to assess the numerical accuracy of Eq. (10), and an empirical bound has been applied as indicated in the discussion of the control section of the program (see Section V).

The use of the Encke method is advantageous because the perturbation $\mathbf{P}$ enters the derivatives in Eq. (11) to more significant digits than in the corresponding ones in Eq. (5), and hence the effect of $\mathbf{P}$ is more accurately represented; step size may be increased by about a factor of two over Cowell if a dominant central body is chosen; and the differential equations are such that numerical stability of the Adams-Moulton predictor is not quite the problem that it is when Cowell derivatives are used, even though both methods use one application of Adams-Moulton corrector to insure ultimate stability. A comparison of the numerical results appears in Section III.

C. Solutions to the Two-Body Problem

As mentioned in the preceding section, for Encke's method it is necessary to obtain a solution to the two-body problem as a function of time. At epoch T_0, in general, a set of osculating elements is required, defined by $\mathbf{R}_0$, $\mathbf{V}_0$, and the equations of motion

$$\ddot{\mathbf{R}} = -\frac{\mu\mathbf{R}}{R^3} \tag{12}$$

Observe that $\mathbf{R} \times \mathbf{V}$ is a constant vector since

$$\begin{aligned} \frac{d(\mathbf{R}\times\mathbf{V})}{dt} &= \frac{d(\mathbf{R}\times\dot{\mathbf{R}})}{dt} = \dot{\mathbf{R}}\times\dot{\mathbf{R}} + \mathbf{R}\times\ddot{\mathbf{R}} \\ &= -\frac{\mu}{R^3}(\mathbf{R}\times\mathbf{R}) = \mathbf{0} \end{aligned}$$

$c_1 = |\mathbf{R}\times\mathbf{V}|$, the angular momentum, is defined as a constant of the motion. In the exposition below, $c_1 \neq 0$ is assumed; if the osculating elements give $c_1 \approx 0$, then a nonosculating set is used for the Encke program so that c_1 is clearly defined. Next

$$\mathbf{W} = \frac{\mathbf{R}\times\mathbf{V}}{c_1}$$

is defined so the motion is constrained to the plane defined by $\mathbf{W}$. The quantity $c_3 = V^2 - 2\mu/R$ is another constant of the motion

$$\frac{dc_3}{dt} = \frac{d}{dt}\left(\dot{\mathbf{R}}\cdot\dot{\mathbf{R}} - \frac{2\mu}{R}\right) = 2\left\{\ddot{\mathbf{R}}\cdot\dot{\mathbf{R}} + \frac{\mu\dot{R}}{R^2}\right\}$$

$$= 2\left\{-\frac{\mu\mathbf{R}}{R^3}\cdot\dot{\mathbf{R}} + \frac{\mu R\dot{R}}{R^3}\right\}$$

$$= 2\left\{-\frac{\mu\mathbf{R}}{R^3}\cdot\dot{\mathbf{R}} + \frac{\mu\mathbf{R}\cdot\dot{\mathbf{R}}}{R^3}\right\}$$

$$= 0$$

Thus, $c_3 = V^2 - 2\mu/R$ is defined as the "energy" constant.

It is possible now to solve the problem of the motion in the orbital plane defined by $\mathbf{W}$.

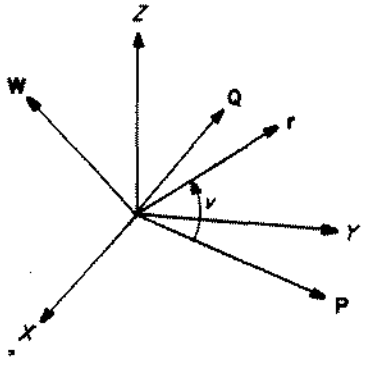

Sketch 2. Two-body orbit

Referring to Sketch 2, let the closest approach distance be q at the epoch T_p, and $\mathbf{P}$ defined as $\mathbf{R}_{min} = q\mathbf{P}$; define $\mathbf{Q} = \mathbf{W}\times\mathbf{P}$ so that a Cartesian coordinate system defined by $\mathbf{P}$ and $\mathbf{Q}$ may be set up in the orbital plane. If R = constant, then $T_p = T_0$. Polar coordinates may be used to write $\mathbf{r} = (x, y) = re^{iv}$, where v is the true anomaly. Note that since

$$\dot{\mathbf{r}} = \dot{r}e^{iv} + ie^{iv}r\dot{v} = \dot{r}e^{iv} + r\dot{v}e^{i(v+\pi/2)}$$

calculate $c_1 = r^2\dot{v}$, since the component $\dot{r}e^{iv}$ of the velocity lies along $\mathbf{r}$ and, hence, does not contribute to the cross product which defines c_1. Finally, by differentiating $\dot{\mathbf{r}}$ and comparing with Eq. (12),

$$\ddot{\mathbf{r}} = \left(\ddot{r} - \frac{c_1^2}{r^3}\right)e^{iv} = -\frac{\mu}{r^2}e^{iv}$$

or

$$\ddot{r} + \frac{\mu}{r^2} - \frac{c_1^2}{r^3} = 0$$

Making the classical change of variables, $1/u = r$, and solving for the geometric orbit with the true anomaly v,

$$\frac{d^2u}{dv^2} + \left(u - \frac{1}{p}\right) = 0$$

where $p = c_1^2/\mu$.

Measuring the initial conditions at epoch T_p, where $v = 0$, the solution has the form

$$u - \frac{1}{p} = \frac{\varepsilon}{p}\cos v$$

since $du/dv = 0$ at $v = 0$. In terms of r, the fundamental geometric solution becomes

$$r = \frac{p}{1 + \varepsilon\cos v} \tag{13}$$

while $q(1 + \varepsilon) = p$; $\varepsilon \geqq 0$ since $p \geqq q$.

An expression for ε is now obtained:

$$V^2 = \dot{r}^2 + \frac{c_1^2}{r^2};\ \dot{r} = \frac{\varepsilon c_1\sin v}{p}$$

$$c_3 = V^2 - \frac{2\mu}{r} = \frac{\mu}{p}(\varepsilon^2\sin^2 v + \varepsilon^2\cos^2 v - 1) \tag{14}$$

$$\varepsilon^2 - 1 = \frac{pc_3}{\mu}$$

$$\varepsilon = \sqrt{1 + \frac{pc_3}{\mu}}$$

The solution may then be expressed as

$$\mathbf{R} = \frac{p\cos v}{1 + \varepsilon\cos v}\mathbf{P} + \frac{p\sin v}{1 + \varepsilon\cos v}\mathbf{Q}$$

$$\mathbf{V} = \frac{-c_1\sin v}{p}\mathbf{P} + \frac{c_1(\varepsilon + \cos v)}{p}\mathbf{Q} \tag{15}$$

At the osculation epoch T_0, from Eq. (13)

$$\cos v_0 = \frac{1}{\varepsilon}\left(\frac{p}{R_0} - 1\right)$$

and by manipulation of Eq. (15)

$$\sin v_0 = \frac{1}{\varepsilon}\frac{p}{R_0 c_1}\mathbf{R}_0\cdot\mathbf{V}_0$$

Inverting Eq. (15) gives the vector expressions

$$\mathbf{P} = \cos v_0\frac{\mathbf{R}_0}{R_0} - \sin v_0\frac{\mathbf{W}\times\mathbf{R}_0}{R_0}$$

$$\mathbf{Q} = \sin v_0\frac{\mathbf{R}_0}{R_0} + \cos v_0\frac{\mathbf{W}\times\mathbf{R}_0}{R_0} \tag{16}$$

Equation (16) is satisfactory only for $\varepsilon \neq 0$; if $\varepsilon = 0$, it is customary to take

$$\mathbf{P} = \frac{\mathbf{R}_0}{R_0}$$

$$\mathbf{Q} = \mathbf{W} \times \mathbf{P}$$

To solve the dynamics, one approach is to work with v, the true anomaly, in the form $w = \tan v/2$.

$$R = \frac{q(1+w^2)}{1+\lambda w^2}$$

where $\lambda = (1-\varepsilon)/(1+\varepsilon)$, in terms of the new variable w.

From the relation $c_1 = R^2 \dot{v}$,

$$\frac{c_1}{2q^2} d T = \frac{1+w^2}{(1+\lambda w^2)^2} dw$$

or

$$g(T - T_p) = \int_0^w \frac{1+u^2}{(1+\lambda u^2)^2} du \qquad (17)$$

where $g = c_1/2q^2$.

In practice, the quadrature on the right side of Eq. (17) is obtained for small values of λ by expanding the integrand as a power series in λ and u^2 and integrating term by term. The resultant form appears in the discussion of subroutine PERI (see Appendix). Equation (15) may be rewritten in terms of w as

$$\begin{aligned} \mathbf{R} &= \frac{1-w^2}{1+\lambda w^2} q \mathbf{P} + \frac{2w}{1+\lambda w^2} q \mathbf{Q} \\ \mathbf{V} &= \frac{-c_1(1+\lambda)w}{q(1+w^2)} \mathbf{P} + \frac{c_1(1-\lambda w^2)}{q(1+w^2)} \mathbf{Q} \end{aligned} \qquad (18)$$

To complete the solution, it is necessary to obtain T_p. If $w_0 = \sin v_0/(1+\cos v_0)$ and λ are not too large, then λw_0^2 will be sufficiently small so that T_p may be calculated from Eq. (17) with the series expansion. It may turn out that λw_0^2 is not suitable, in which case T_p is computed using the eccentric anomaly which is described below. But once T_p is obtained, Eq. (17) may be solved at epoch T by iteration to give w, used to obtain the coordinates as in Eq. (18). Since λw^2 must be a small parameter for the method to work, the principal application comes when either λ is quite small or the motion is confined to a region near closest approach; the latter alternative gives rise to the name "pericenter" method applied to the above process involving w or v.

Another way to obtain the dynamics is through the introduction of the eccentric anomaly. A singularity appears at $c_3 = 0$ which is adequately handled by the pericenter method, as $c_3 = 0$ implies $\lambda = 0$. Otherwise, the elliptical case is distinguished with $c_3 < 0$ and its eccentric anomaly E, while for $c_3 > 0$ and the eccentric anomaly F, the hyperbolic case is considered.

If $c_3 < 0$, E is defined by

$$\begin{aligned} &R = a(1 - \varepsilon \cos E), 0 \leqq |E| \leqq 180^\circ \\ &a = -\frac{\mu}{c_3} \\ &\dot{E} > 0 \text{ so that } E \gtrless 0 \text{ if } T \gtrless T_p \end{aligned} \qquad (19)$$

By substitution into the equation $c_3 = V^2 - 2\mu/R$,

$$(1 - \varepsilon \cos E)\dot{E} = \sqrt{\frac{\mu}{a^3}} = n$$

or

$$E - \varepsilon \sin E = n(T - T_p) \qquad (20)$$

which is Kepler's equation for an ellipse.

Observing that

$$R = a(1 - \varepsilon \cos E) = \frac{p}{1 + \varepsilon \cos v}$$

and

$$\dot{R} = a\varepsilon \sin E \dot{E} = \frac{\varepsilon c_1}{p} \sin v$$

leads to

$$\begin{aligned} \cos v &= \frac{\cos E - \varepsilon}{1 - \varepsilon \cos E} \\ \sin v &= \frac{\sqrt{1-\varepsilon^2}\sin E}{1 - \varepsilon \cos E} \end{aligned} \qquad (21)$$

Substitution of Eq. (21) into Eq. (15) yields

$$\begin{aligned} \mathbf{R} &= a(\cos E - \varepsilon)\mathbf{P} + a\sqrt{1-\varepsilon^2}\sin E \mathbf{Q} \\ \mathbf{V} &= \frac{-an \sin E}{1 - \varepsilon \cos E} \mathbf{P} + \frac{an\sqrt{1-\varepsilon^2}\cos E}{1 - \varepsilon \cos E} \mathbf{Q} \end{aligned} \qquad (22)$$

E_0 is determined at epoch T_0 by

$$\begin{aligned} \cos E_0 &= \frac{1}{\varepsilon}\left(1 - \frac{R_0}{a}\right) \\ \sin E_0 &= \frac{1}{\varepsilon} \frac{\mathbf{R}_0 \cdot \mathbf{V}_0}{a\sqrt{|c_3|}} \end{aligned}$$

so that T_p may be determined using these equations along with Eq. (20).

To obtain the coordinates at epoch T for the elliptical orbits, Eq. (20) is solved by iteration given in the discussion of subroutine KEPLER (see Appendix).

The hyperbolic case defined by $c_3 > 0$ admits a similar solution. Start with the definition for F

$$R = a\,(e\cosh F - 1)$$

$$a = \frac{\mu}{c_3} \qquad (23)$$

$$\dot{F} > 0 \text{ so that } F \gtreqless 0 \text{ if } T \gtreqless T_p$$

To obtain the form of Kepler's equation for the hyperbola, use c_3 as with the elliptical case, and obtain

$$(e\cosh F - 1)\,\dot{F} = \sqrt{\frac{\mu}{a^3}} = n$$

and Kepler's equation

$$e\sinh F - F = n\,(T - T_p) \qquad (24)$$

Comparing expressions for R and $\dot{R}$, v and F are related by

$$\cos v = \frac{e - \cosh F}{e\cosh F - 1}$$

$$\sin v = \frac{\sqrt{e^2 - 1}\sinh F}{e\cosh F - 1} \qquad (25)$$

Replacing the quantities in Eq. (15) by those in Eq. (25), the expressions for the coordinates become

$$\mathbf{R} = a\,(e - \cosh F)\,\mathbf{P} + a\sqrt{e^2 - 1}\sinh F\;\mathbf{Q}$$

$$\mathbf{V} = \frac{-a n \sinh F}{e\cosh F - 1}\,\mathbf{P} + \frac{a n\sqrt{e^2 - 1}\cosh F}{e\cosh F - 1}\,\mathbf{Q} \qquad (26)$$

At the epoch T_0, T_p may be determined from Eq. (24), when F_0 is obtained from

$$\cosh F_0 = \frac{1}{e}\left(1 + \frac{R_0}{a}\right)$$

$$\sinh F_0 = \frac{1}{e}\,\frac{\mathbf{R}_0 \cdot \mathbf{V}_0}{a\sqrt{c_3}}$$

The iterative solution of Kepler's equation at epoch T is used to obtain the coordinates; the discussion of subroutine QUADKP (see Appendix) describes the numerical technique used for the hyperbolic case.

III. NUMERICAL EXPERIENCE

Trajectories computed using single-precision derivatives calculated in the Encke manner should be slightly more accurate than those generated using the Cowell form of the equations of motion, provided that a proper choice of central body has been made. The difference between the two methods arises from the fact that the relatively small size of the perturbing acceleration, as compared with the central body acceleration, permits the Encke scheme to retain more significance in the total acceleration, as compared with the corresponding acceleration term in the Cowell scheme. It is assumed that the reference orbit for the Encke scheme lies sufficiently close to the true orbit so that the quantity $\rho/R_0 < 0.03$, where $\mathbf{R}_0$ is the position in the reference orbit while $\boldsymbol{\rho}$ is the difference between $\mathbf{R}$, the position in the true orbit, and $\mathbf{R}_0$. Under this assumption, the main term in the acceleration for the Encke method, viz., $-\mu/R_0^3\ (\boldsymbol{\rho} - F(Q)\mathbf{R})$, will in general be at least an order of magnitude smaller than the corresponding Cowell term, $-\mu\mathbf{R}/R^3$, for $F(Q) \approx 3Q = 3\boldsymbol{\rho}\cdot(\mathbf{R}_0 + \boldsymbol{\rho}/2)/R_0^2 \approx 3\rho/R_0$ at worst; thus $|\boldsymbol{\rho}/R_0 - F(Q)\mathbf{R}/R_0| \approx 4\rho/R_0$ and as $R_0^3/R^3 \approx 1 - 2Q$, the ratio of acceleration terms will never exceed 0.12. The ultimate accuracy of the Encke scheme is tied to the accurate solution of the two-body problem for obtaining the reference orbit; less accuracy in the reference orbit would be sufficient for computation of the main Encke acceleration term and a less accurate solution than this would suffice for the perturbations.

Rounding error in the computation of the main Cowell acceleration term propagates into the numerical solution in a strikingly simple fashion—T_p, the epoch of pericenter passage, alone of the orbital elements is significantly perturbed. To demonstrate the effect of roundoff, a high Earth-satellite trajectory was run with both Cowell and Encke schemes; additional information was obtained by successively chopping the last and the last two bits in each coordinate of the acceleration vector at each integration step. A comparison of the effect on the orbital elements at the first perigee point appears in Table 1.

As a measure of the over-all difference in the trajectories, comparison of the difference in range δR may be made near the perigee. Under the assumption that T_p is the only orbital element to be affected, then

$$\delta R = R_2 - R_1 = \delta R^* \frac{\sqrt{1-\varepsilon^2}\sin E^*}{1 - \varepsilon\cos E^*}$$

where

$$E^* = \frac{1}{2}(E_1 + E_2)$$

satisfies the equation

$$E^* - \varepsilon\sin E^* = n(T - T_p^*),$$

$$T_p^* = \frac{1}{2}(T_p^{(1)} + T_p^{(2)})$$

$$\delta R^* = \frac{a n \varepsilon}{\sqrt{1-\varepsilon^2}}\delta T_p$$

$$\delta T_p = T_p^{(2)} - T_p^{(1)}$$

where the superscript 1 refers to a comparison trajectory while the superscript 2 refers to a perturbed trajectory. δR^* is the extreme value of δR occurring at $n(T - T_p^*) = \pm(\cos^{-1}\varepsilon - \varepsilon\sqrt{1-\varepsilon^2})$. A summary of results in Table 2 serves to demonstrate the adequateness of the conic approximation. The small perturbation in T_p contributes only a small difference in the coordinates, if a comparison is made at a greater time from perigee.

Table 1. Orbital elements at perigee

Case	q^a km	ε	$T_p{}^b$ sec	i deg	ω deg	Ω deg
Normal Encke	8901.362	0.98534697	69.077	19.599986	200.94431	222.18236
Encke with last bit chopped	8901.362	0.98534687	69.074	19.599986	200.94431	222.18236
Encke with last two bits chopped	8901.362	0.98534697	69.088	19.599986	200.94431	222.18235
Normal Cowell	8901.425	0.98534641	22.029	19.600052	200.94427	222.18245
Cowell with last bit chopped	8901.420	0.98534644	27.063	19.600039	200.94428	222.18243
Cowell with last two bits chopped	8901.402	0.98534650	38.793	19.600027	200.94429	222.18241

[a]Closest approach distance.

[b]Time of pericenter passage, past $45^d\ 12^h\ 58^m$ after the injection epoch.

As a further comparison of the Encke and Cowell methods, three lunar trajectories were selected which had flight times of 35 hr, 45 hr, and 66 hr, respectively. The trajectories were characterized by an injection altitude of about 200 km near perigee and a termination of 1738.09 km from the center of the Moon. Table 3 compares results obtained by the running of each trajectory four different ways: (1) Encke, Moon-centered second phase; (2) Encke, Earth-centered second phase; (3) Cowell, Moon-centered second phase; and (4) Cowell, Earth-centered second phase. In all instances the second phase was started at a distance of 30,000 km from the center of the Moon. It appears from the data that all four methods are consistent and yield results of satisfactory accuracy.

The 66-hr lunar trajectory was used to estimate the effect of integrating in a coordinate system based on the true equator and equinox of date. A precise comparison is impossible, since injection conditions expressed in the of-date system must be rotated to the mean equator and equinox of 1950.0 for integration in the normal case. Such an operation introduces a small variation in the injection coordinates which propagates under integration into the numerical solution, thus partially masking the difference between the two coordinate systems. However, an estimate of the variational effect was made which could account for about half of the observed difference in the Cartesian coordinates at lunar encounter. The perturbations in these coordinates, arising solely from the two different coordinate systems for integration, seem therefore to amount to about 1 km; in addition, the flight time received a perturbation amounting to about 0.6 sec. These differences appear to be significant when viewed in the light of the data in Table 3.

As interplanetary trajectories are usually run in three phases—phase one Earth-centered, phase two Sun-centered, and phase three target-centered—it is necessary

Table 2. Range differences near perigee

Case	δR at $45^d\ 12^h$ km		δR at $45^d\ 14^h$ km		Maximum δR km	
	Computed[a]	Observed[b]	Computed[a]	Observed[b]	Computed[a]	Observed[b]
Encke with last bit chopped minus normal Encke	−0.014	−0.014	0.014	0.010	0.014	0.014
Encke with two bits chopped minus normal Encke	0.050	0.052	−0.050	0.052	0.051	0.053
Normal Cowell minus normal Encke	−215.028	−214.943	213.824	213.705	220.168	220.064
Cowell with last bit chopped minus normal Cowell	23.025	23.017	−22.860	−22.850	23.557	23.548
Cowell with two bits chopped minus normal Cowell	76.661	76.631	−76.144	−76.103	78.450	78.413

[a]Values derived from the orbital elements.
[b]Values derived from the normal trajectory output.

Table 3. Comparison of lunar trajectories

Case	Lunar Impact Time	B · T[a] km	B · R[a] km	i[a] deg
35^h Encke E-M	$1^d\ 10^h\ 53^m\ 08\overset{s}{.}619$	44.129	9.785	27.3383
35^h Encke E-E	$1^d\ 10^h\ 53^m\ 08\overset{s}{.}624$	44.142	9.785	27.3384
35^h Cowell E-M	$1^d\ 10^h\ 53^m\ 08\overset{s}{.}620$	44.139	9.787	27.3347
35^h Cowell E-E	$1^d\ 10^h\ 53^m\ 08\overset{s}{.}625$	44.149	9.787	27.3341
45^h Encke E-M	$1^d\ 20^h\ 51^m\ 32\overset{s}{.}279$	19.017	14.500	46.8673
45^h Encke E-E	$1^d\ 20^h\ 51^m\ 32\overset{s}{.}284$	19.042	14.499	46.8322
45^h Cowell E-M	$1^d\ 20^h\ 51^m\ 32\overset{s}{.}279$	19.031	14.499	46.8475
45^h Cowell E-E	$1^d\ 20^h\ 51^m\ 32\overset{s}{.}287$	19.047	14.500	46.8408
66^h Encke E-M	$2^d\ 17^h\ 49^m\ 03\overset{s}{.}028$	270.281	−88.532	37.1864
66^h Encke E-E	$2^d\ 17^h\ 49^m\ 03\overset{s}{.}047$	270.324	−88.536	37.1848
66^h Cowell E-M	$2^d\ 17^h\ 49^m\ 03\overset{s}{.}064$	270.300	−88.565	37.1906
66^h Cowell E-E	$2^d\ 17^h\ 49^m\ 03\overset{s}{.}078$	270.339	−88.571	37.1894

[a]The orbital elements B · T and B · R are computed along with i, the inclination, at the time the distance 1738.09 km from the center of the Moon is reached.

at the change into phase two to compute the velocity of the Sun by numerical differentiation of position coordinates, which is inaccurate on two counts: first, the position ephemeris of the Sun displays noise in the seventh figure of the positions, which gives rise to inconsistencies in the velocities as obtained from neighboring segments of the ephemeris; second, even with eight-figure accuracy in the position data, calculation of the velocities entails differencing so that significant figures are lost.

To determine the magnitude of the error introduced in the velocity coordinates as used for normal cases, an 80-day arc of the Earth's orbit was smoothed by a least-squares fit which utilized a numerical integration of the equations of motion. Residuals on the order of two units in the seventh figure of the position coordinates were obtained by the fitting process. As a by-product of the fit, smooth velocity coordinates were obtained which were therefore consistent with the new position coordinates. Intermediate values of the velocities were then obtained by both a numerical differentiation of the new position ephemeris and a direct interpolation of the velocity ephemeris; a comparison of the results revealed maximum differences of about 0.02 m/sec, or discrepancies in the seventh figure. Next, the original noisy position coordinates were differentiated and compared with the interpolation in the velocity ephemeris. In this case, the maximum differences were observed to be about 0.15 m/sec, or a relative error of about 5×10^{-6}.

An actual Venus trajectory with a flight time of 108 days was studied for the effect of inaccuracies introduced in the velocity transformation in the transfer to phase two by the systematic variation of the epoch of the coordinate change, and also by running a trajectory which integrated heliocentrically all the way to Venus encounter. The results are summarized in Table 4, which gives the deviation of coordinates at the fixed epoch of transfer into phase two, and of the time of Venus encounter, all referred to the standard trajectory which used the ordinary phasing. The differences in the coordinates may be explained quite well by the known magnitude of maximum error in the velocity of the Sun and the value of the appropriate partial coefficients. The trajectory, which was integrated all the way to Venus in phase one, does not suffer from the velocity problem, but because the noisy position coordinates used in the calculation of the now large perturbations in the acceleration undoubtedly contribute a significant amount of error in the solution, this technique does not solve the accuracy problem.

Encke and Cowell methods for the interplanetary case are compared by running Venus and Mars trajectories in which the transfer point from phase one to phase two was kept fixed for the respective trajectories. Evidently, the difference between the two methods shows up more distinctly the longer the flight time, but is of acceptable magnitude, as Table 5 indicates.

In summary, the trajectory program gives consistent single-precision results for the Encke and Cowell meth-

Table 4. Differences at transfer to Venus-centered phase

Transfer time[a]	δX Mm[b]	δY Mm[b]	δZ Mm[b]	δTF sec
93.50	0.6	0.1	0.0	78
93.75	−0.1	0.0	0.0	−15
94.00	−0.7	−0.1	0.0	−87
94.25	−1.2	−0.1	0.0	−140
94.50	−1.2	−0.1	0.1	−132
94.75	−1.4	−0.2	0.1	−155
95.00	−1.6	−0.2	0.1	−181
95.25	−1.8	−0.3	0.1	−211
95.50	−1.9	−0.4	0.0	−234
95.75	−2.2	−0.5	0.0	−370
96.00	−2.3	−0.7	−0.1	−503
96.25	−2.4	−0.9	−0.2	−332
96.50	−2.7	−1.1	−0.2	−381
96.75	−2.7	−1.3	−0.3	−403
97.00	−2.7	−1.4	−0.4	−420
97.25	−2.7	−1.5	−0.4	−434
97.50	−2.9	−1.6	−0.5	−461
97.75	−2.8	−1.7	−0.6	−467
98.00	−2.7	−1.8	−0.7	−470
98.25	−2.6	−1.9	−0.7	−472
98.50	−2.0	−1.9	−0.7	−417
All geocentric	0.6	−1.0	−0.5	−37

[a]The transfer time represents the Julian date in E.T. at which entry was made into the heliocentric phase.
[b]Megameters.

Table 5. Comparison of interplanetary trajectories

Case	TF[a] sec	B · T[b] km	B · R[b] km	i, deg
108[d] Venus, Encke	51.279	−4120.9	1694.4	153.9196
108[d] Venus, Cowell	56.636	−4120.5	1693.2	153.9295
118[d] Venus, Encke	25.236	249632.8	−630020.9	76.8357
118[d] Venus, Cowell	26.827	249629.9	−630022.0	76.8359
231[d] Mars, Encke	9.743	−50153.6	−4537.4	173.4127
231[d] Mars, Cowell	34.938	−50205.4	−4541.3	173.4134

[a]The time of flight is measured from an arbitrary epoch.
[b]The orbital elements are calculated either at planetary encounter or at closest approach.

ods, but the ephemeris problem for interplanetary flight presents a source of systematic error. This problem will be largely eliminated by a study now in progress at the Jet Propulsion Laboratory to obtain smoothed position and velocity ephemerides which are gravitationally consistent.

IV. OPERATING INSTRUCTIONS AND DESCRIPTION OF INPUT

A. Operation of the Space Trajectories Program on the IBM 7090

The Space Trajectories Program is designed to accept offline card input in BCD on tape A2, to prepare an offline BCD output tape on A3, and to obtain ephemeris information from a tape mounted on A8 assumed to be written in high density. For operational convenience, the offline output may be monitored on the online printer by depressing sense switch 6, which permits simultaneous off- and online output. The other sense switches, the sense lights, the panel keys, and the sense indicator register are not used; additionally, the floating-point trapping mode of execution is not used.

A machine run usually consists of several cases which are defined by the appropriate case parameters punched on cards in a format accepted by the 7090 version of NYINPI, a SHARE input routine. The sets of cards which define individual cases are separated by TRA 3,4 cards, and each set may be trailed by its package of phase cards to complete the input for running the trajectory. A description of the available case parameters appears in Sections IVD-1 and D-2.

For the normal type of "minimum print" trajectory, a set of phase parameters suitable for the case may be selected from the parameters assembled in the program to be used for the standard targets Earth, Moon, Venus, and Mars. The values of the stored parameters appear in Section IVF. Complete control over the trajectory may be obtained by the appropriate choice of phase parameters for each sequential phase belonging to the case; the phase parameters read in are saved and may be used for subsequent cases so that one run might consist of several cases, all using a common set of phase cards which is read in but once. The functions of the specific parameters used in a phase are described in Sections IVE-2 and E-3.

B. Basic Coordinate Systems

The fundamental coordinate system used by the Space Trajectories Program for reference of the equations of motion is the Cartesian frame formed by the mean equator and equinox of 1950.0; the position of the mean equator of the Earth and the ascending node of the mean orbit of the Sun on that equator, taken at the beginning of the Besselian year 1950, serve as the definition. The X axis is directed along the node, the Z axis northward above the equator, and the Y axis in a direction to complete the usual right-handed coordinate system. The auxiliary reference frame based on the Earth's mean equator of date, and the mean equinox of date defined by the Sun's mean orbit about the Earth (ecliptic of date), may be obtained from the 1950.0 system by the application of the precession as described in the discussion of subroutine ROTEQ (see Appendix).

Reference to the Earth's true equator of date is obtained by the rotation of the mean equator of date about the mean equinox of date to the ecliptic of date via the mean obliquity of date, rotation in the ecliptic to form the true equinox of date via the nutation in longitude, and, finally, the rotation about the true equinox by means of the true obliquity of date formed by augmenting the mean obliquity by the nutation in obliquity. The three rotations described result in but a small change, hence the mean and true coordinates in general agree through the first four figures. The description of subroutine NUTATE (see Appendix) contains formulas for the rotation matrix which performs the necessary transformation from mean coordinates to true.

C. Coordinate Systems for Input

Provisions have been made to input directly into the Cartesian equatorial system of 1950.0 the basic coordinate frame for the numerical integration. A simple rotation about the mean vernal equinox of 1950.0, with magnitude the mean obliquity of 1950.0, permits input in the mean equinox and ecliptic of 1950.0. With the aid of the nutations in longitude and obliquity, along with the general precession, it becomes possible to input in either the true equator and equinox of date or the true equinox and ecliptic of date. The Cartesian coordinates expressed in any one of the above four systems may refer to one of the six available bodies Earth, Moon, Sun, Venus, Mars, and Jupiter.

It is convenient to input the injection conditions in a spherical set associated with one of the Cartesian coordinate systems which describes the position vector in terms of range and two angles, and the velocity vector corresponding as velocity (speed) and two angles. For this purpose, the Cartesian frame is regarded as being at rest in the case of the true of-date systems; the reference frame may be thought of as being "osculating" rather than

undergoing a slow rotation in inertial space and thus forming a rotating coordinate system. The set of equations necessary for the transformation from sphericals to Cartesian, along with the definitions of the angles, may be found in the description of subroutine RVIN (Appendix).

The Earth-fixed spherical set of injection conditions is based on a Cartesian coordinate system assumed to rotate with the Earth: the $x - y$ plane coincident with the Earth's true equator of date, the x axis lying in the Greenwich meridian, and the z axis along the Earth's spin axis. As described in subroutine GHA (Appendix), a formula is furnished which gives the Greenwich hour angle of the true vernal equinox of date so that the Earth-fixed Cartesian coordinates may be referred to the true equator and equinox of date via a simple rotation. Of course, the velocity vector in the Earth-fixed system is affected by the Earth's rotational rate; appropriate formulas for the velocity transformation to the nonrotating system are given in subroutine EARTH (Appendix).

A similar treatment of the Moon gives rise to injection conditions expressed in selenographic (Moon-fixed sphericals) coordinates; formulas for the position of the Moon's true equator, the prime meridian of selenographic longitude reference, and the rotation of the Moon are contained in the discussion of subroutines XYZDD, MNA, and MNAMD (Appendix).

A final input coordinate system, based on orbital elements of an escape hyperbola from the Earth, completes the number of options. The hyperbola has been characterized by its ascending asymptote given by right ascension and declination, by the energy, and by the constraint that the launch site lie in the orbital plane. The actual shape of the hyperbola and the injection point are given by the remaining two parameters, the path angle and the range at the injection time.

The equations for the energy-asymptote input option may be developed as illustrated in the following:

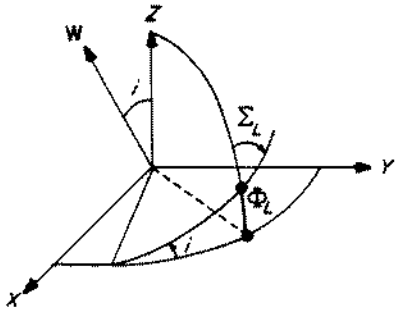

Sketch 3. Launch geometry

Given Σ_L, the azimuth at the launch site, as in Sketch 3,

$$W_z = \cos i = \sin \Sigma_L \cos \Phi_L$$

where $\Phi_L = 28.309$ deg, the latitude of the launch site, a program parameter.

$$\mathbf{S} = (\cos \Phi_S \cos \Theta_S, \cos \Phi_S \sin \Theta_S, \sin \Phi_S),$$

the ascending asymptote

$$W_y = \frac{-W_z \sin \Theta_S \sin \Phi_S - \cos \Theta_S \sqrt{\cos^2 \Phi_S - W_z^2}}{\cos \Phi_S}$$

If the radicand is negative, the error message

"DECLINATION OF ASCENDING ASYMPTOTE OUT OF RANGE"

is printed and the trajectory is aborted.

$$W_x = -\frac{S_y W_y + S_z W_z}{S_x},$$

completing the construction of **W**, the unit angular momentum vector.

$V = \sqrt{c_3 + \frac{2\mu_\oplus}{R}}$, the velocity

$c_1 = |\mathbf{R} \times \mathbf{V}| = RV \cos \Gamma$, the angular momentum

$\varepsilon^2 - 1 = \frac{c_3 c_1^2}{\mu_\oplus^2}$, for the eccentricity

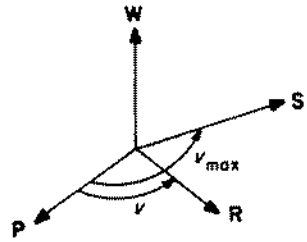

Sketch 4. Relationship of ascending asymptote and perigee

From $\sin \Gamma = \varepsilon \sin (v - \Gamma)$, invert to obtain $-90° < v - \Gamma < 90°$ and v, the true anomaly. In particular, for $\Gamma = 90°$, an expression for v_{max}, the maximum true anomaly (Sketch 4) is

$$\nu_{max} = \cos^{-1}\left(-\frac{1}{\epsilon}\right), \quad 90° < \nu_{max} < 180°$$

$$\mathbf{R} = R\{\cos(\nu_{max} - \nu)\,\mathbf{S} + \sin(\nu_{max} - \nu)\,\mathbf{S} \times \mathbf{W}\}$$

The velocity vector (Sketch 5) is given by

$$\mathbf{V} = V\left\{\cos\Gamma\frac{\mathbf{W} \times \mathbf{R}}{R} + \sin\Gamma\frac{\mathbf{R}}{R}\right\}$$

completing the construction of the Cartesian coordinates.

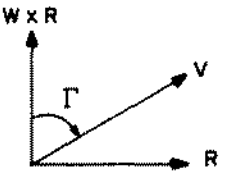

Sketch 5. Description of the velocity vector

D. Relationship Between Case Analysis and Phase Analysis

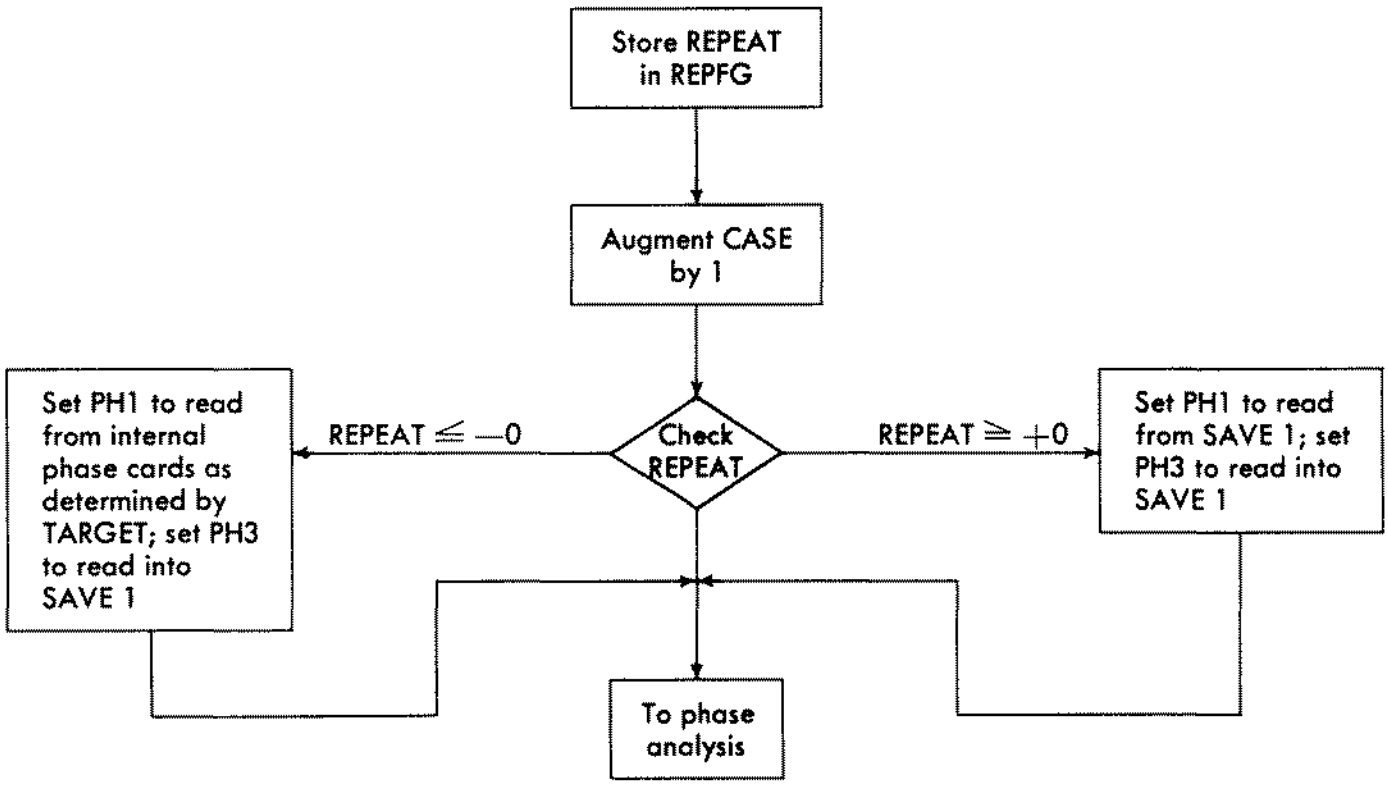

For CASE ANALYSIS, input desired value of CASE and REPEAT.

If REPEAT = ±0, all phase cards are read in and buffered at the same time.

Phase 1 cards
TRA 3,4
.
.
.
Last phase cards
TRA 3,4

} Stack of phase cards for all phases to be read in for the present case

Observe that the symbolic address card

CASE O −1

may be used to effect (CASE) = 0 at the phase-analysis point of the program.

D. (Cont'd)

1. Case Parameters

Input location (decimal)	*Class field*	*Program name*	*Identification*
100–109	BCD	60-character comment field printed at top of each page of output	
110	BCD	TARGET	BCD name of target body
111	BCD	KERN	BCD name of central body at injection
112	OCT	REPEAT	Phase input control word
113	OCT	INJECT	Injection input type
114–115	DEC	T1	Injection epoch in sexagesimal format
116–118	DEC	X1, Y1, Z1	Injection coordinates identified by INJECT
119–121	DEC	X1., Y1., Z1.	
122	DEC	GAMMAC	Thrust attitude angles giving fixed direction of thrust vector
123	DEC	SIGMAC	
124	DEC	ACC1	Thrust magnitude in lb force
125	DEC	MASS1	Initial mass in lb
126	DEC	MASS.1	Mass flow rate in lb/sec
127	DEC	TBO1	Duration of burning in sec
128–129	DEC	TGO1	Epoch for ignition of motor
136	DEC	RADP	Coefficient for radiation pressure
137	OCT	FLAGS	Bit 34 = integrate frequency equations Bit 35 = integrate variational equations
138	DEC	T(K)	Single-precision floating-point time
139	BCD	EQUNOX	Injection equator and equinox

2. Detailed Description of Case Parameters

Program name	*Explanation*
TARGET	May be Earth, Moon, Sun, Venus, Mars, or Jupiter. It is used to define the target quantities in the various print groups and to select the appropriate set of minimum phase cards when REPEAT $\leqq -0$ and the target is neither the Sun nor Jupiter.
KERN	May be any of the bodies as used with TARGET. KERN defines the central body of the coordinate system at injection and may be distinct from the central body of integration for phase one.
REPEAT	Determines whether or not phase input cards are to follow:

Value of REPEAT	Effect
−1	Does not input phase cards but uses one of the four internal sets as determined by TARGET.

D2. (Cont'd)

Program name		*Explanation*
	−0	Uses the internal sets of phase cards as with REPEAT = −1; modifications are read in on top of working buffer, and altered phase parameters are stored in a special buffer to be used later. After last cards for the last phase have been read in, REPEAT is set to +1.
	+0	Similar to REPEAT = −0 but does not make use of any internally stored phase cards.
	+1	Assumes all phases have been previously loaded and uses appropriate buffer for input.

INJECT

The seven available types are as follows:

Value of INJECT	Coordinate System
+0	Inertial Cartesian, equatorial
−0	Inertial Cartesian, ecliptic
+1	Inertial spherical, equatorial
−1	Inertial spherical, ecliptic
+2	Earth-fixed spherical
+3	Selenographic (spherical)
+4	Energy-asymptote Earth-centered equatorial

Note: For INJECT = ±0 or ±1, coordinate system may be modified by EQUNOX

T1

Double precision epoch of injection in the two-word fixed-point decimal format which is denoted by "sexagesimal format."

Format of the two words is

yymmoddhh,nnssfff

where the fields are

yy = year, e.g., 61 for 1961

mm = month, e.g., 11 for November

odd = day, 3-digit field, where zero must appear before digits for day of month

hh = hours past start of day

nn = minutes

ss = seconds

fff = milliseconds

Note: This epoch is modified by T(K).

D2. (Cont'd)

Program name	*Explanation*	
X1, Y1, Z1, X1., Y1., Z1.	Value of INJECT	Interpretation
	+0	**R** and **V** in equatorial Cartesian coordinates
	−0	**R** and **V** in ecliptic Cartesian coordinates
	+1	R, Φ, Θ; V, Γ, Σ inertial equatorial spherical coordinates
	−1	R, β, λ; V, Γ, Σ inertial ecliptic spherical coordinates
	+2	r, ϕ, θ; v, γ, σ Earth-fixed spherical
	+3	$r_{\mathbb{C}}$, $\phi_{\mathbb{C}}$, $\theta_{\mathbb{C}}$; $v_{\mathbb{C}}$, $\gamma_{\mathbb{C}}$, $\sigma_{\mathbb{C}}$ selenographic (spherical) coordinates
	+4	Σ_L, R, Γ; c_3, Φ_S, Θ_S energy-asymptote in Earth-centered equatorial system

Interpretation is modified by EQUNOX below. Position units are km, velocity units are km/sec, and angles are in deg.

GAMMAC, SIGMAC — At injection the position vector **R** is formed. A fixed-thrust attitude vector **C** is characterized by the path angle γ_c and the azimuth angle σ_c with respect to a plane perpendicular to **R** and the Z axis as a reference direction. **R** may be a body-fixed vector so that γ_c and σ_c would have a different interpretation if the selenographic input option were used rather than Moon-centered Cartesian, for instance.

For powered-flight computation the following formula is used for the acceleration with the parameters described below:

$$\mathbf{a} = \frac{-F}{m_0 - \dot{m}(T - T_0)}\mathbf{C} \text{ for } T_0 \leqq T \leqq T_0 + t_b$$

ACC1 — F, thrust in lb force; internally multiplied by $g = 0.0098$ to obtain a in km/sec²

MASS1 — m_0, initial mass in lb

MASS.1 — $\dot{m}$, mass flow rate in lb/sec

TBO1 — t_b, duration of burning in floating-point sec

TGO1 — T_0, epoch of motor ignition in sexagesimal format as with T1, or the modified sexagesimal format as with PRTEND in Section IVE-3.

Further phase control must be provided for the powered flight as indicated in the flow diagrams of the phase logic (Section V) and the description of the phase parameters; i.e., there must be a phase to start the motor.

For radiation pressure calculation the following equation is used:

$$\mathbf{a} = \frac{Ag}{W} K\alpha^2 \frac{\mathbf{R}_{sp}}{R^3_{sp}}$$

where

α = number of km/A.U., included to make $\alpha^2\mathbf{R}_{sp}/R^3_{sp}$ dimensionless

D2. (Cont'd)

Program name	*Explanation*
	$\mathbf{R}_{sp}$ = the Sun-probe vector $K = 1.03034 \times 10^{-8}$ lb force/m², the solar-flux constant A = effective area in m² W = mass of spacecraft in lb $g = 0.0098$, conversion factor to express acceleration in km/sec² internally
RADP	Ag/W with units as above, m²-km/sec² lb force
FLAGS	The two low-order bits are used to control the introduction of the 10 frequency equations ($b_{34} = 1$) and the 36 variational equations ($b_{35} = 1$) for numerical integration in the Jet Propulsion Laboratory tracking program.
T(K)	After T1 is converted internally to double-precision floating-point sec past 0^h January 1, 1950, T(K) is added on to give the effective injection time.
EQUNOX	If the BCD field is all blanks, then the input is regarded as being expressed in the true equator and equinox of date or the true ecliptic and equinox of date. Otherwise the reference is the mean system of 1950.0. As EQUNOX is displayed along with the injection conditions, it is customary to use the six characters "1950.0" for the latter case. The data for case parameters describing the injection conditions and powered-flight parameters and the associated control is terminated by the card TRA 3,4. Further cases may follow unless the phase-card input is triggered via REPEAT = ±0. In that event, of course, all the necessary cards for the various phases must follow, then the subsequent cases.

E. Phase-Card Reading and Buffering

1. Storage Layout of Internal Buffers

Input locations
140 to 179

USE buffer

USE buffer
mapped onto SAVE
buffers ↔ REPEAT = ±0

$SAVE_1$
$SAVE_{10}$

10 buffers

Nominal phase cards stored in core:

☾

⊕	phase 1
☾	phase 2

☿

⊕	phase 1
⊙	phase 2
☿	phase 3

♂

⊕	phase 1
⊙	phase 2
♂	phase 3

⊕

⊕	phase 1
⊙	phase 2
⊕	phase 3

☾ Moon
⊙ Sun
☿ Venus
♂ Mars
⊕ Earth

2. Phase Parameters

Location	*Type field*	*Program name*	*Description*
140	OCT	LAST	Controls last phase and some of the print
141	BCD	REND	Body used to form R_{sp}
142	DEC		Value of R_{sp} used to terminate phase
143	BCD	REND.	Body used to form $\dot{R}_{sp}$
144	DEC		Suppression distance from central body

E2. (Cont'd)

Location	*Type field*	*Program name*	*Description*
145	OCT	MODE	Integrate Encke or Cowell
146	BCD	CENTER	Central body for integration
147–148	DEC	H	Initial step size, modified sexagesimal format
149	OCT	DOUBLE	Number of initial doubles
150	BCD	HKERN	Body from which to compute step sizes
151–162	DEC	PRTEND, DELPRT	3 print end times and intervals
163–166	DEC	ODDPRT	2 odd-print epochs
167	OCT	GROP	12-octal-character field to control print groups
168–169	OCT	CODE1	24-octal-character field for station prints
170–171	OCT	VIEW	24-octal-character field for stations for view periods
178	OCT	ORBETT	Reference for $\mathbf{B} \cdot \mathbf{T}$ and $\mathbf{B} \cdot \mathbf{R}$ in conic output
179	BCD	EQUNX1	Output equator and equinox

3. **Detailed Description of Phase Parameters**

Program name	*Explanation*
LAST	sgn { − = call PRINTD at $T\phi$; + = don't call PRINTD at $T\phi$
	bit 33 { 0 = reset T_{PRT} to $T\phi$ at start of phase ; 1 = use old T_{PRT} from previous phase
	bit 34 { 0 = call PRINTD at end of phase ; 1 = don't call PRINTD at end of phase
	bit 35 { 0 = last phase ; 1 = more phases to follow

PRINTD is the subroutine which prints the selected groups.

T_{PRT} is the print epoch constructed in the previous phase which would have been reached for printing had the previous phase extended in time to T_{PRT}.

When new phase cards are being read, bit 35 = 0 also flags the end of the reading process.

$T\phi$ is the epoch at change of phase.

E3. (Cont'd)

Program name	*Explanation*
REND REND.	End-of-phase devices: A phase may be terminated by one of the following three conditions: 1. R_{END} 2. $\dot{R}_{END}$ 3. T_{END} 1. R_{END}: The BCD name of the body to which R_{END} refers is input in 141; the desired value $R_{np} = R_{END}$ is input in 142. R_{END} is used as a dependent variable stop. 2. $\dot{R}_{END}$: The BCD name of the body from which $\dot{R}_{VP}$ is measured is input in 143; 144 is interpreted as: (1) (REND. + 1) = 0: suppress $\dot{R}$ test (2) (REND. + 1) $\neq$ 0: test effective in the following ways: a. If CENTER = TARGET, stop at $\dot{R} = 0$ via a dependent variable stop b. If CENTER $\neq$ TARGET, suppress test until: *1.* $R >$ (REND. + 1) if (REND. + 1) > 0; or *2.* $R <$ |(REND. + 1)| if (REND. + 1) < 0 R refers to the central body. 3. T_{END}: $T_{END} = \max(T\phi, T_{END_1}, T_{END_2}, T_{END_3})$ where the T_{END_i}'s are the end of print times input in 151, 155, and 159 and $T\phi$ is the epoch of phase change.
MODE	0 = integrate the equations of motion as developed for a Cowell scheme 1 = integrate Encke's modification of the equations of motion
CENTER	Any of the six bodies may be used as the central body; but for R_{END} and $\dot{R}_{END}$ the following bodies are available: Central Body — Perturbing Bodies Earth — Moon, Sun; Jupiter if $R > 10^6$ km Moon — Earth, Sun Sun, Venus, Mars, Jupiter — All remaining bodies
H	Adams-Moulton step size in modified sexagesimal format: yy = 0 and mm = 0, so that the remainder is converted to sec. If (H), (H + 1), and (DOUBLE) = 0, the step size is selected automatically as a function of HKERN and is halved or doubled under program control as the need arises.

E3. (Cont'd)

Program name	*Explanation*
DOUBLE	If (H) or (H + 1) $\neq 0$, a fixed-point number in this field gives the number of times the step is to be doubled consecutively.
HKERN	Selects the body from which the step size is to be computed; resultant calculated step size is used for other purposes so that HKERN is effective even though (H) or (H + 1) $\neq 0$.
PRTEND, DELPRT	The 12 input locations are divided into three 4-word fields giving control over print intervals: $T_{END_1}, \Delta T_{PRT_1}; T_{END_2}, \Delta T_{PRT_2}; T_{END_3}, \Delta T_{PRT_3}$ The T_{END_i} may be input as epochs in the usual sexagesimal format or as intervals past injection expressed in the modified sexagesimal format in which yy = mm = 0. In the latter event, the epoch T_{END_i} is formed by augmenting the injection epoch by the interval. The ΔT_{PRT_i} are intervals as represented in the modified sexagesimal format. If T_{END_i} is input as zero, it is replaced by a large number but is ignored in the calculation of T_{END}. Finally the T_{END_i} are internally sorted and consequently need not be input in ascending sequence. The location for T_{END_2} is PRTEND + 4 or DELPRT + 2, since PRTEND and DELPRT define the first of the two words in T_{END_1} and ΔT_{PRT_1} respectively.
ODDPRT	T_{ODD_1} and T_{ODD_2} are input to provide execution of PRINTD without interrupting the main printing sequence. The format is the same as for T_{END_i} and the two resultant epochs are sorted as before. $T_{ODD_i} = 0$ is replaced by a large number.

Treatment of print times:

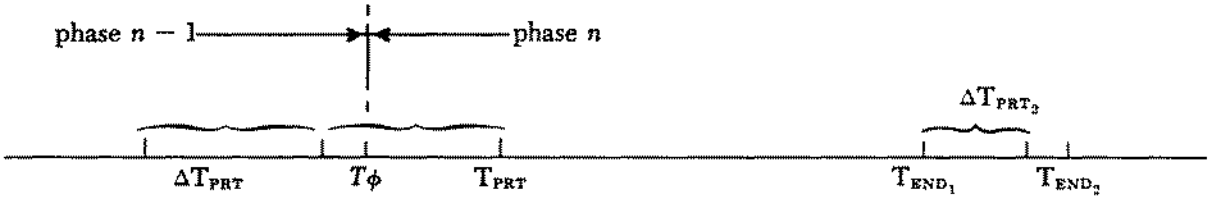

At time of entry to the new phase, T_{PRT} is the next print time as determined by phase $n - 1$. If the print reset option is chosen, $T_{PRT_0} = T\phi$ will be the first print time. Otherwise,

$$T_{PRT_0} = \min \{T_{PRT}, T_{END_1}\}$$

No matter how T_{PRT_0} is chosen,

$$T_{PRT_1} = \begin{cases} \min \{T_{PRT_0} + \Delta T_{PRT_1}, T_{END_1}\}, \text{ if } T_{END_1} > T_{PRT_0}; \\ \min \{T_{END_1} + \Delta T_{PRT_2}, T_{END_2}\} \text{ otherwise} \end{cases}$$

Thus the T_{END_i}'s function is to reset the printing interval and print epoch. $T\phi$ is the time at which the nth phase starts.

E3. (Cont'd)

Program name	*Explanation*

GROP

The 12 octal characters of GROP are mapped onto the 12 words GROPS + 0, · · · , GROPS + 11:

GROPS	+0	geocentric
	+1	geocentric conic
	+2	heliocentric
	+3	heliocentric conic
	+4	spacecraft and powered flight
	+5	target
	+6	target conic
	+7	print at $\dot{R} = 0$ (central body only)
	+8, +9, +10, +11	not used

The 3 bits of the octal digits have the following use:

bit 1 { 0 = print effective whenever called
1 = print effective as a function of the status of phase

bit 2 { 0 = print only when the start-of-phase condition holds } holds for bit 1 = 1; ignore if bit 1 = 0
1 = print only when the end-of-phase condition holds }

bit 3 { 0 = ecliptic output
1 = equatorial output

Special cases are:

1. All bits zero → don't print group
2. Configuration = $3)_8$, same as (1) above

At $\dot{R} = 0$ print, the value in GROPS + 7 is mapped onto the cell for the central body conic and PRINTD is executed.

Start of phase means the first time that PRINTD is called in the phase unless the end-of-phase condition has been met at that time.

End of phase means that phase has been terminated by one of the following conditions:

1. R_{END} attained
2. $\dot{R}$ test fulfilled
3. T_{END} attained

E3. (Cont'd)

Program name	*Explanation*
CODE1	Only the leftmost 15 octal characters of the two input words are used. 0 = suppress station, 1 = include station. At print time, station print is suppressed if $\gamma_i < -10°$

The 15 stations are, in order:

1. Antigua
2. Ascension
3. Millstone Hill
4. Mobile Tracker
5. A.M.R. G.E. Tracker
6. Bermuda
7. Goldstone Receiver
8. Goldstone Transmitter
9. Grand Bahama Island
10. Johannesburg
11. Hawaii
12. Jodrell Bank
13. Puerto Rico
14. San Salvador
15. Woomera

VIEW

Printouts of the station occur at $\dot{\gamma}_i = 0$, provided $\gamma_i \geqq \gamma_0$, and at $\gamma_i = \gamma_0$, where γ_0 may be input by the symbolic card

STACRDD-001 γ_0

Enough triggers have been provided to take care of a maximum of five stations.

Provisions have been made for symbolic card input of station coordinates and names if necessary.

STABCD

0-3} Station 1 name
4-7} Station 2 name
•
•
•

STACRD

$0\ \phi_1$
$1\ \theta_1$
$2\ r_1$
$3\ f_{B_1}$
$4\ f_{C_1}$
} Station 1
•
•
•

ORBETT

If 0, uses **T** lying in the orbital plane of body concerned. If 1, uses **T** lying either in the equatorial or ecliptic, as called for by the conic GROPS location.

The orbital planes are defined as follows:

Body:	Orbital Plane With Respect to:
Earth	Sun
Moon	Earth
Sun	Earth
Venus	Sun
Mars	Sun
Jupiter	Sun

E3. (Cont'd)

Program name	*Explanation*
EQUNX1	If blank, output is referred to true equator or ecliptic and equinox of date; otherwise, the reference is to the mean equator or ecliptic and equinox of 1950.0. Normally the BCD "1950.0" is used here when mean equator or ecliptic and equinox of 1950.0 is desired.

The cards representing input for the phase parameters for a given phase are terminated by a TRA 3,4 card. The last phase cards read in are indicated by a zero in the low-order bit of the parameter LAST.

F. Standard Phases

Standard phases are available for the Moon, Earth, Venus, and Mars as the target. The words TARGET and REPEAT in the case parameters control the use of the stored parameters.

If REPEAT = −1, the standard phases are used.

If REPEAT = −0, the standard phases are used but modifications may be read in to replace the stored parameters.

The stored values of the standard phases are listed in the following:

1. Stored Phase Cards for Moon as Target

Location	*Type field*	*Phase 1*	*Phase 2*
140	OCT	−1	0
141	BCD	MOON	MOON
142	DEC	30E3	1738.09
143	BCD	MOON	MOON
144	DEC	330E3	1E3
145	OCT	1	1
146	BCD	EARTH	MOON
147	DEC	0,0,0	0,0,0
150	BCD	EARTH	MOON
151	DEC	15 00,0	20 00,0
153	DEC	15 00,0	20 00,0
155	DEC	0,0,0,0	0,0,0,0
159	DEC	0,0,0,0	0,0,0,0
163	DEC	0,0,0,0	0,0,0,0
167	OCT	55 00 0 00 00 000	11 20 1 11 00 000
168	OCT	0,0	0,0
170	OCT	0,0	0,0
178	OCT	0	0
179	BCD	blank	blank

F. (Cont'd)

2. Stored Phase Cards for Earth as Target

Location	*Type field*	*Phase 1*	*Phase 2*	*Phase 3*
140	OCT	−1	−1	0
141	BCD	EARTH	EARTH	EARTH
142	DEC	2.5E6	2.4E6	6378.
143	BCD	EARTH	EARTH	EARTH
144	DEC	0	152E6	1E3
145	OCT	1	1	1
146	BCD	EARTH	SUN	EARTH
147	DEC	0,0,0	0,0,0	0,0,0
150	BCD	EARTH	SUN	EARTH
151	DEC	140 00,0	190 00,0	200 00,0
153	DEC	140 00,0	190 00,0	200 00,0
155	DEC	0,0,0,0	0,0,0,0	0,0,0,0
159	DEC	0,0,0,0	0,0,0,0	0,0,0,0
163	DEC	0,0,0,0	0,0,0,0	0,0,0,0
167	OCT	55 00 0 00 00 000	00 22 0 00 00 000	10 20 0 01 00 000
168	OCT	0,0	0,0	0,0
170	OCT	0,0	0,0	0,0
178	OCT	0	0	0
179	BCD	blank	blank	blank

3. Stored Phase Cards for Venus as Target

Location	*Type field*	*Phase 1*	*Phase 2*	*Phase 3*
140	OCT	−1	−1	0
141	BCD	EARTH	VENUS	VENUS
142	DEC	2.5E6	2.5E6	6100.
143	BCD	VENUS	VENUS	VENUS
144	DEC	0	−110E6	1E3
145	OCT	1	1	1
146	BCD	EARTH	SUN	VENUS
147	DEC	0,0,0	0,0,0	0,0,0
150	BCD	EARTH	SUN	VENUS
151	DEC	20 00,0	190 00,0	200 00,0
153	DEC	20 00,0	190 00,0	200 00,0
155	DEC	0,0,0,0	0,0,0,0	0,0,0,0
159	DEC	0,0,0,0	0,0,0,0	0,0,0,0
163	DEC	0,0,0,0	0,0,0,0	0,0,0,0
167	OCT	55 00 0 00 00 000	00 22 0 00 00 000	10 20 0 22 00 000
168	OCT	0,0	0,0	0,0

F3. (Cont'd)

Location	*Type field*	*Phase 1*	*Phase 2*	*Phase 3*
170	OCT	0,0	0,0	0,0
178	OCT	0	0	1
179	BCD	blank	blank	blank

4. Stored Phase Cards for Mars as Target

Location	*Type field*	*Phase 1*	*Phase 2*	*Phase 3*
140	OCT	−1	−1	0
141	BCD	EARTH	MARS	MARS
142	DEC	2.5E6	2E6	3415.
143	BCD	MARS	MARS	MARS
144	DEC	0	240E6	1E3
145	OCT	1	1	1
146	BCD	EARTH	SUN	MARS
147	DEC	0,0,0	0,0,0	0,0,0
150	BCD	EARTH	SUN	MARS
151	DEC	20 00,0	250 00,0	270 00,0
153	DEC	20 00,0	250 00,0	270 00,0
155	DEC	0,0,0,0	0,0,0,0	0,0,0,0
159	DEC	0,0,0,0	0,0,0,0	0,0,0,0
163	DEC	0,0,0,0	0,0,0,0	0,0,0,0
167	OCT	55 00 0 00 00 000	00 22 0 00 00 000	10 20 0 22 00 000
168	OCT	0,0	0,0	0,0
170	OCT	0,0	0,0	0,0
178	OCT	0	0	1
179	BCD	blank	blank	blank

V. FLOW CHARTS AND METHOD OF CONTROL

A. Control in the Space Trajectories Program

After the necessary transformation of the injection conditions to the Cartesian coordinates based on the mean equator and equinox of 1950.0, the Space Trajectories Program is controlled primarily by the subroutine MARK (see Appendix) which performs the stepwise numerical integration of the equations of motion to obtain the solution at desired points along the trajectory. The trajectory is divided into phases to permit control of output format and print frequency and of the numerical integration process itself. Each phase is characterized by a set of phase parameters which are interpreted before the numerical integration proceeds.

During numerical integration in a phase, the derivatives are requested by MARK; the derivative routine provides the necessary information and also performs the calculation of the auxiliary dependent variables which MARK might need as requested by the associated dependent variable triggers. The end-of-step routine monitors the numerical process by computing the step size and communicating this information to MARK, by control of rectification, and by determination of closest approach to a noncentral body.

At the print times, as determined by the triggers to MARK, the requested output groups are printed as described in Section VI.

B. General Flow in Space Trajectories Program

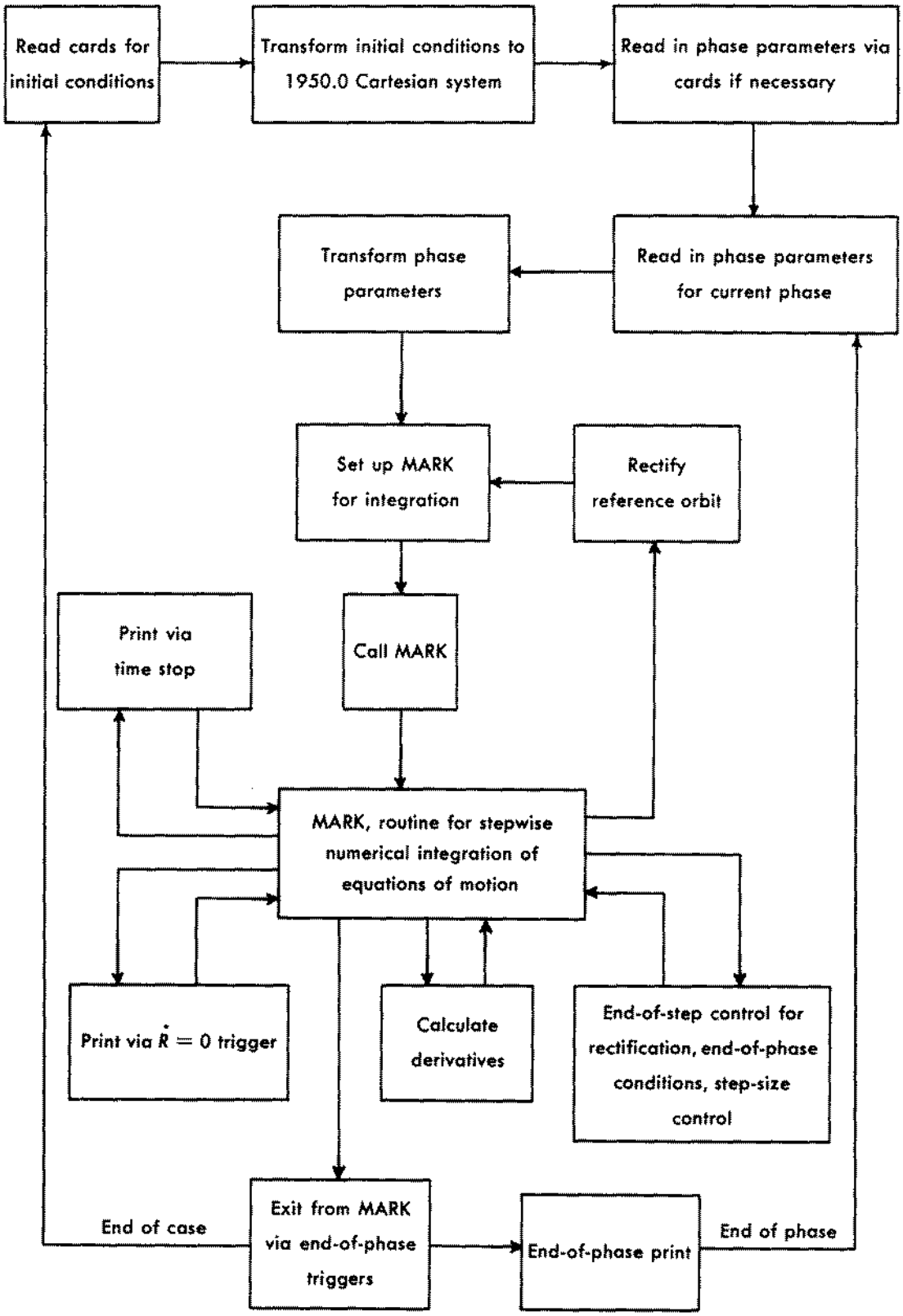

C. Flow During Transformation of Injection Conditions

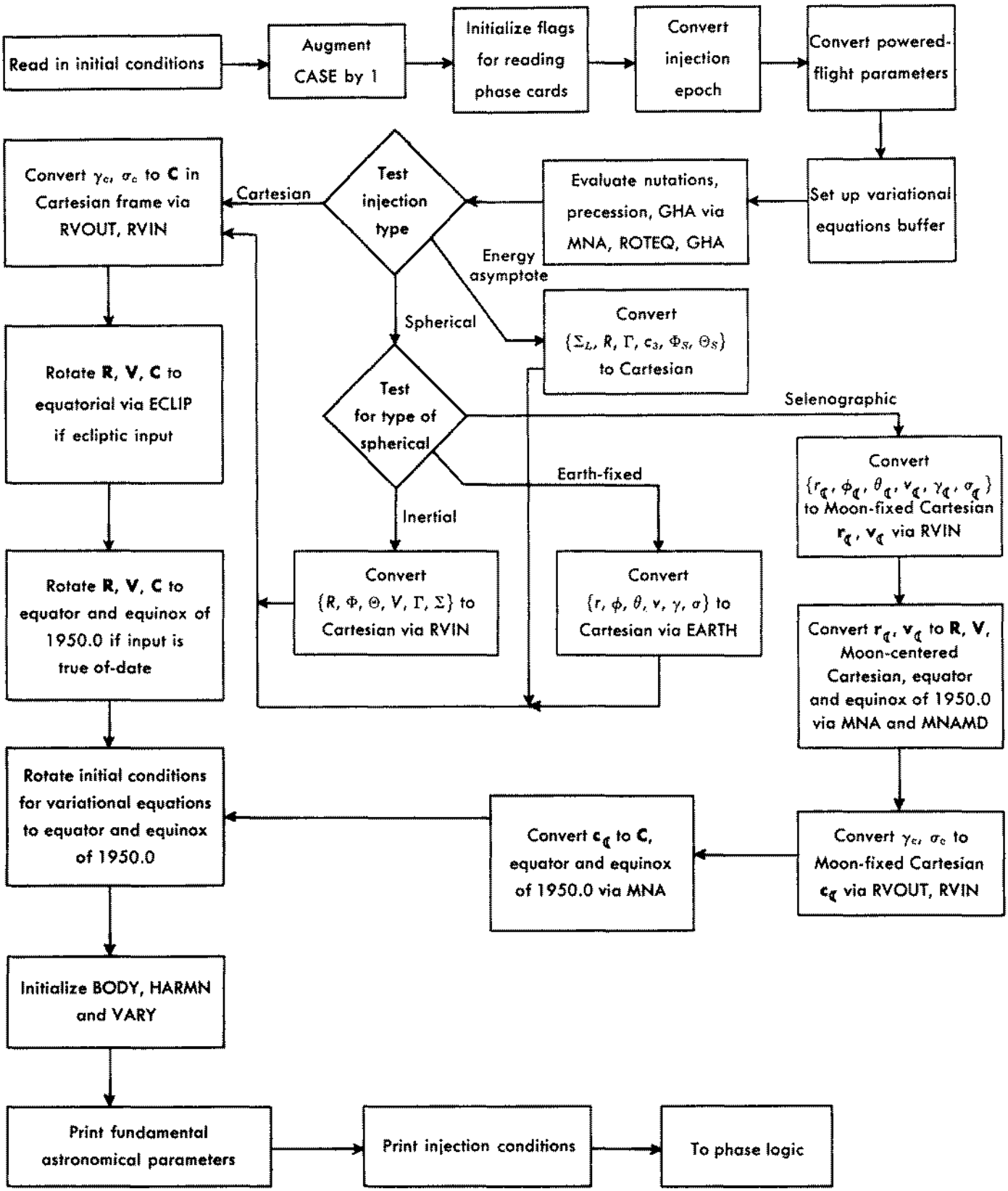

D. Flow During Transfer of Phase Parameters

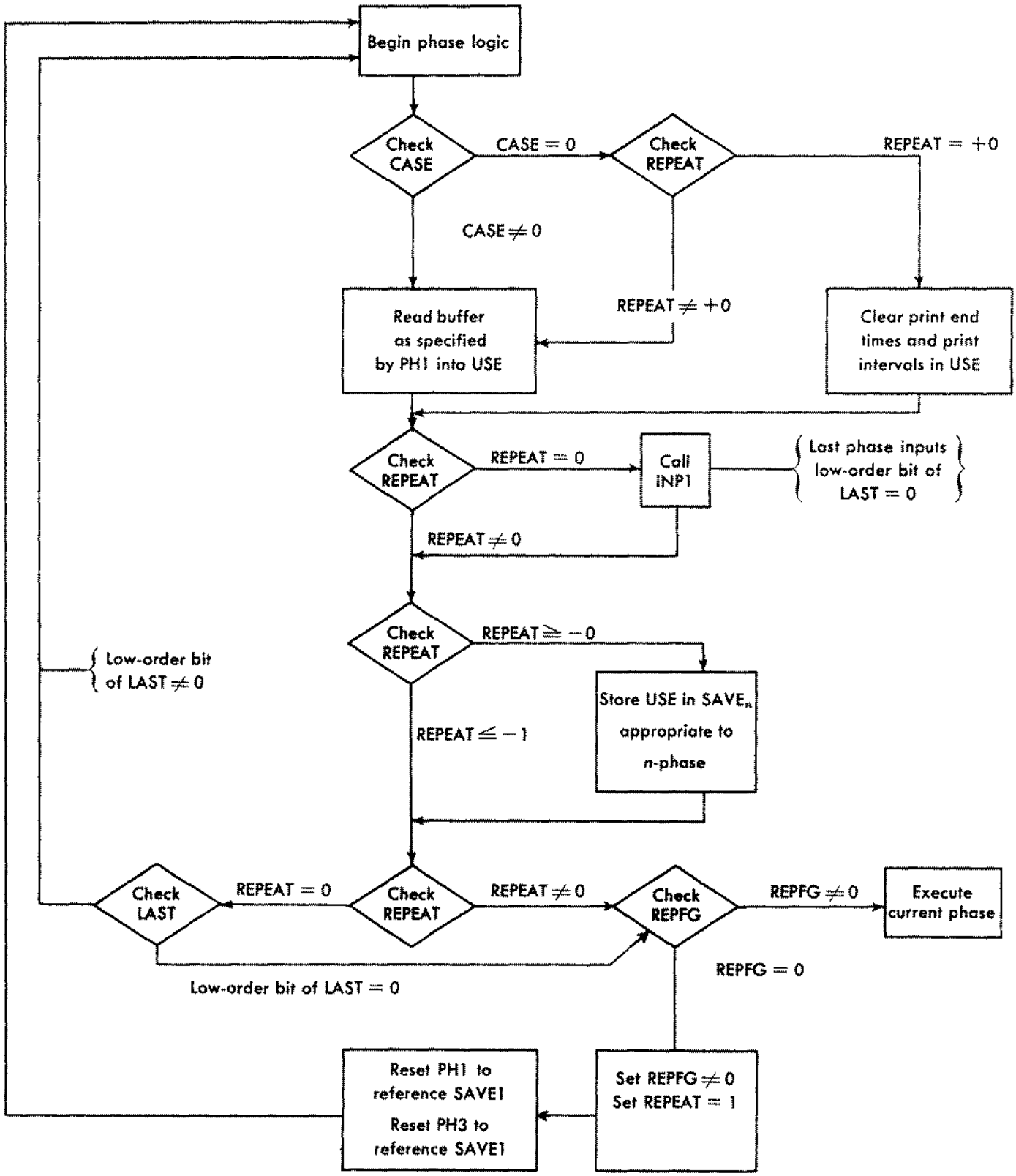

E. Flow in Phase Setup

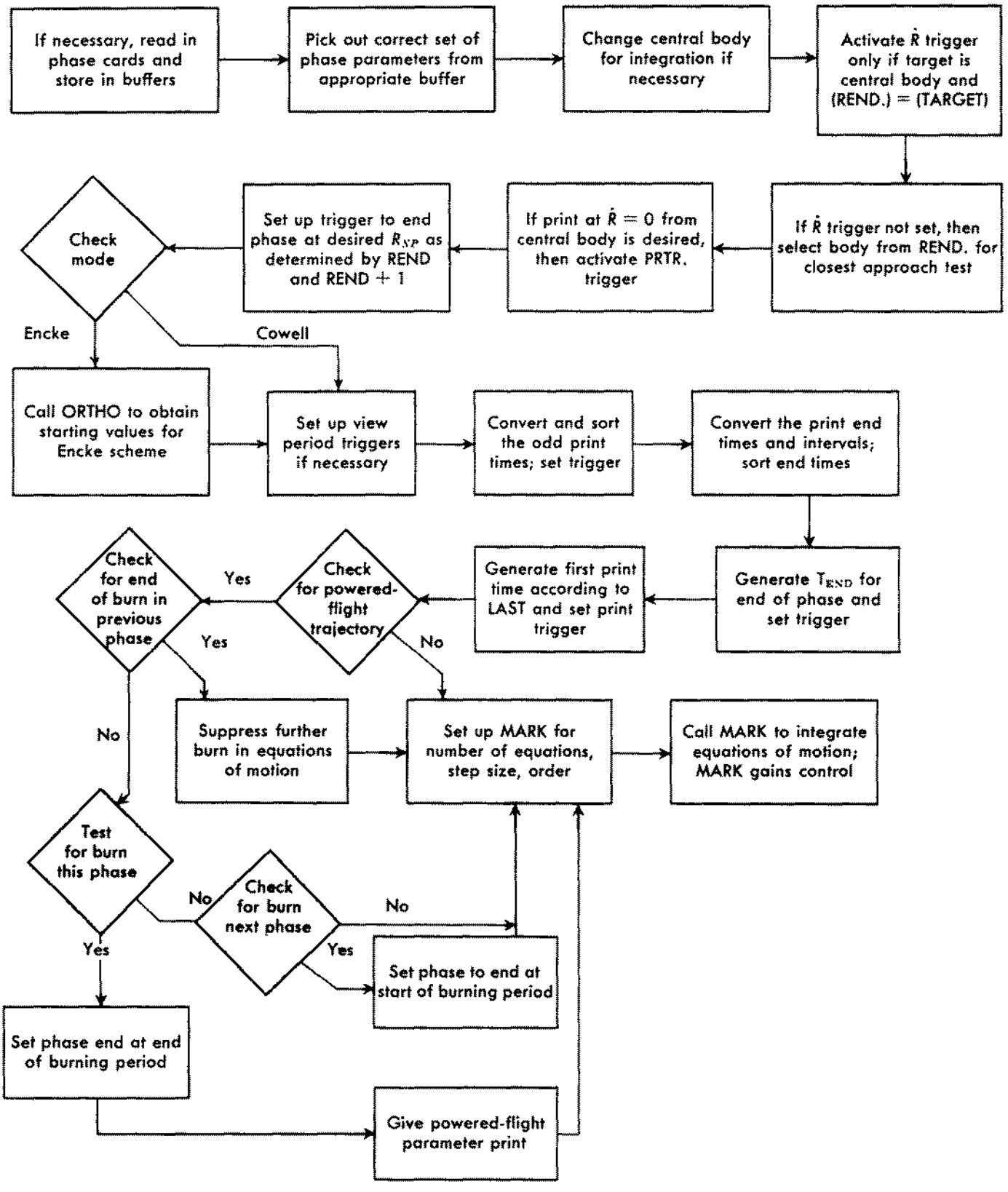

F. End-of-Step Logic

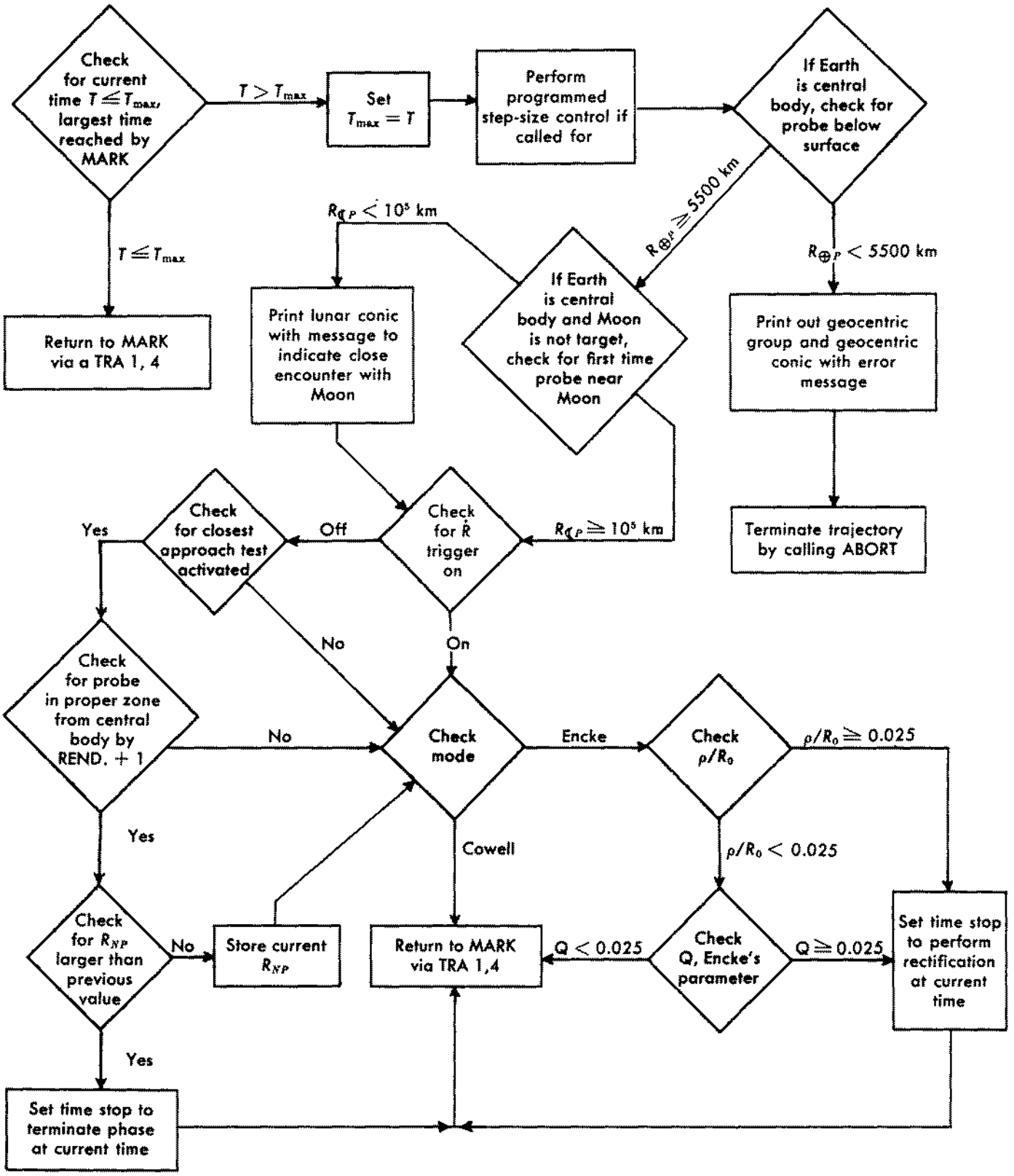

G. Function of the Derivative Routine

The derivative routine DOT assumes the COMMON storage layout for the following quantities; coordinates are in the mean equator and equinox of 1950.0.

Symbol	*Storage*	*Explanation*
T	BSS 2	Double-precision time in sec past 0^h January 1, 1950, U.T.
CX, CY, CZ		$\mathbf{R}$ if Cowell, $\boldsymbol{\rho}$ if Encke
CX., CY., CZ.		$\mathbf{V}$ if Cowell, $\dot{\boldsymbol{\rho}}$ if Encke
VAR	BSS 36	Solution of the variational equations $\frac{\partial \mathbf{R}}{\partial X_0}, \frac{\partial \dot{\mathbf{R}}}{\partial X_0}, \frac{\partial \mathbf{R}}{\partial Y_0}, \cdots, \frac{\partial \mathbf{R}}{\partial \dot{Z}_0}, \frac{\partial \dot{\mathbf{R}}}{\partial \dot{Z}_0}$
	BSS 3	Derivative of $\mathbf{R}$ if Cowell, of $\boldsymbol{\rho}$ if Encke; placed in buffer by DOT from CX., CY., CZ.
CX.., CY.., CZ..		$\ddot{\mathbf{R}}$ if Cowell, $\ddot{\boldsymbol{\rho}}$ if Encke; computed by DOT and placed in buffer
VAR.	BSS 36	Derivatives of quantities appearing in the VAR buffer; $\partial\ddot{\mathbf{R}}/\partial X_0, \cdots, \partial\ddot{\mathbf{R}}/\partial \dot{Z}_0$ computed by DOT and placed in buffer; remaining quantities are selected from the VAR buffer; final order is $\frac{\partial \dot{\mathbf{R}}}{\partial X_0}, \frac{\partial \ddot{\mathbf{R}}}{\partial X_0}, \frac{\partial \dot{\mathbf{R}}}{\partial Y_0}, \cdots, \frac{\partial \ddot{\mathbf{R}}}{\partial \dot{Y}_0}, \frac{\partial \dot{\mathbf{R}}}{\partial \dot{Z}_0}, \frac{\partial \ddot{\mathbf{R}}}{\partial \dot{Z}_0}$
QX, QY, QZ		$\mathbf{R} = \mathbf{R}_0 + \boldsymbol{\rho}$ if Encke, same as contents of CX, CY, CZ if Cowell; placed in buffer by DOT
QX., QY., QZ.		$\mathbf{V} = \mathbf{V}_0 + \dot{\boldsymbol{\rho}}$ if Encke, same as the contents of CX., CY., CZ. if Cowell; placed in buffer by DOT only if velocity needed
QX0, QY0, QZ0		$\mathbf{R}_0$, position solution to the two-body orbit; calculated by ENCKE only when in Encke mode
QX0., QY0., QZ0.		$\mathbf{V}_0$, velocity solution to the two-body orbit; calculated by SPEED only when velocity is necessary in the Encke mode

H. Flow in the Derivative Routine

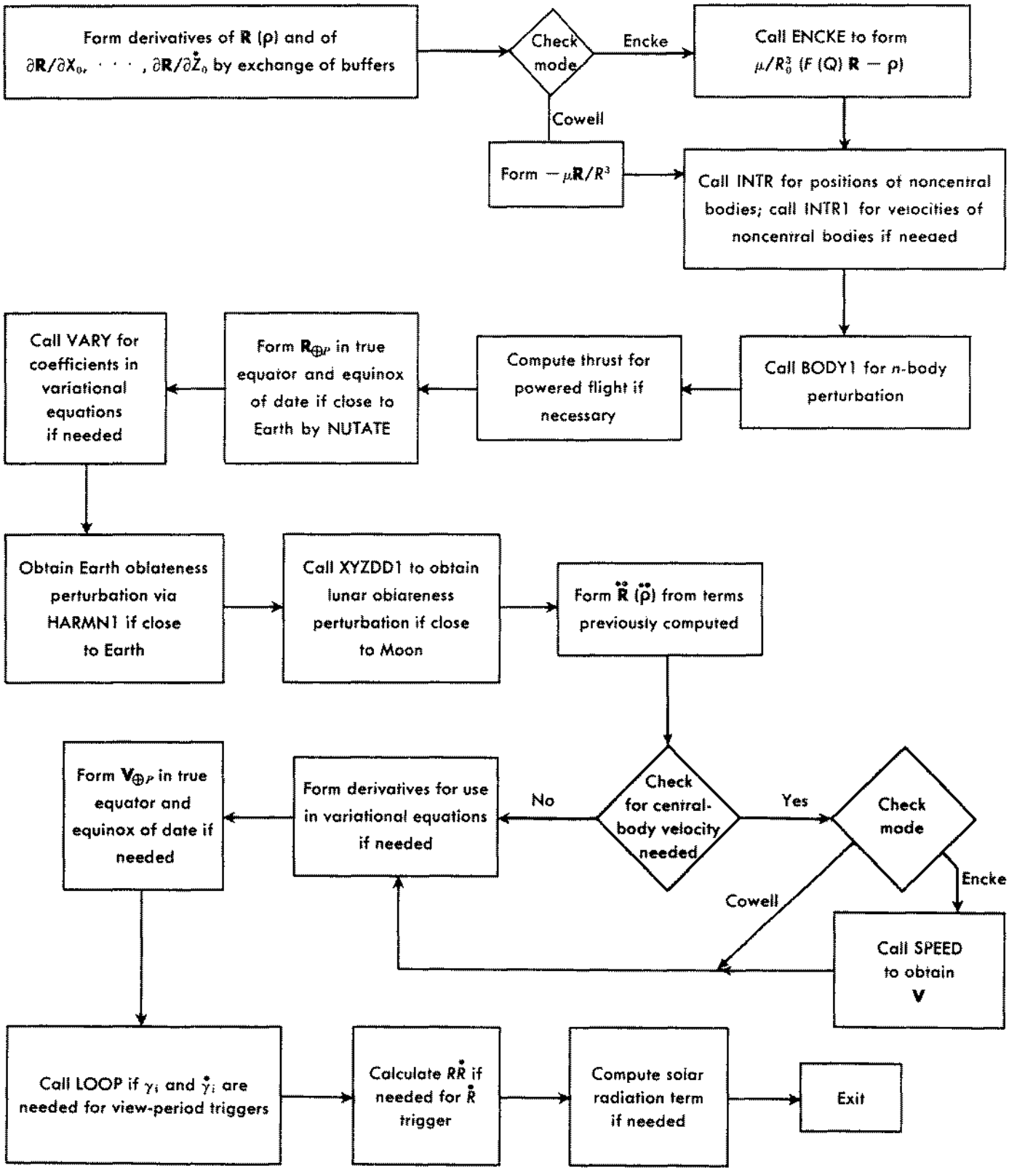

I. Automatic Step-Size Control

Step-size control is provided as a function of the range from a selected body during a particular phase. For this purpose each body has associated with it a list of range intervals; the step size remains constant during a particular interval and is doubled for the next higher interval. For the lowest interval there is defined an h_{min}; all other step sizes chosen will therefore be of the form $h = 2^n h_{min}$.

At the start of the integration MARK uses Runge-Kutta for the first m steps. Therefore, at the onset, $h_0 = \frac{1}{4}h_c$ is set in HBANK while HBANK1 is set to 2; after m Runge-Kutta steps and $2m$ Adams-Moulton steps, MARK would be using $h = 4h_0$ for its next step. The control section permits the Runge-Kutta steps to be carried out before attempting to modify the step size to new h_c.

Assuming MARK is using Adams-Moulton for the integration, h_c is computed at the end of each step and compared with h, the value MARK is using. If $h_1 = 2^k h$, where k is the number of uncompleted doubles, then the following tests are made:

1. $h_c = h_1$: No action to be taken
2. $h_c > h_1$: Augment HBANK1 by the number of additional doubles necessary to make $h = h_c$ and call ABTB to let MARK pick up the additional doubles. Record the change.
3. $h_c < h = h_1$: Augment HBANK2 by number of halves necessary to make $h = h_c$ and call ABTB to let MARK pick up the additional halves. Record the change. $h = h_1$ was indicated by the fact that HD = 0.
4. $h_c \leqq h < h_1$: Set ND = HBANK1 = 0 and wait until HD = 0 at a later integration step. Save number of necessary halves and execute (3) when $h = h_1$, i.e., when HD = 0.
5. $h < h_c < h_1$: Let MARK double up to h_c by altering both HBANK1 and ND. Record change and continue, but do not call ABTB.

It is to be noted that controlling step size in the above manner does not produce instantaneous changes in the current MARK step h. Therefore, a conservative choice of values has been made in the range lists to insure stability of the numerical solution in all the practical cases which have arisen. Each h_{min} for the planets has been chosen to give good results for a low-altitude satellite whose orbit is to be calculated using an Encke scheme.

If a Cowell scheme is to be used, the program sets $h'_{min} = h_{min}/2$; thus the step-size regimen consists of a precise and uniform halving of all step sizes in the range intervals; automatic halving and doubling are consequently executed in general in a shorter time span in the Cowell mode.

The base step-size and range lists are accessible via the symbolic input location H((0)). The exact internal structure follows:

Location	*Value, sec*	*Explanation*
− 6	120	♅
− 5		not used
− 4	60	♂
− 3	60	♀
− 2	43,200	☉
− 1	60	☾
H((0)) − 0	60	⊕

Range list for Earth and Venus

Location	*Value, km*
H((0)) + 1	10^{20}
+ 2	2.8×10^6
+ 3	1.8×10^6
+ 4	10^6
+ 5	600,000
+ 6	400,000
+ 7	120,000
+ 10	80,000
+ 11	30,000
+ 12	16,000
LST00 = H((0)) + 13	8,000

Range list for Mars

Location	*Value, km*
H((0)) + 14	10^{20}
+ 15	2×10^{6}
+ 16	1.2×10^{6}
+ 17	800,000
+ 20	500,000
+ 21	300,000
+ 22	100,000
+ 23	60,000
+ 24	25,000
+ 25	12,000
LST04 = H((0)) + 26	6,000

Range list for Moon

Location	*Value, km*
H((0)) + 27	10^{20}
+ 30	70,000
+ 31	45,000
+ 32	30,000
+ 33	20,000
+ 34	12,000
LST01 = H((0)) + 35	5,000

Range list for Jupiter

Location	*Value, km*
H((0)) + 36	10^{20}
+ 37	5×10^{6}
+ 40	3×10^{6}
+ 41	2×10^{6}
+ 42	1.2×10^{6}
+ 43	10^{6}
+ 44	800,000
+ 45	600,000
+ 46	400,000

Range list for Jupiter (cont'd)

Location	*Value, km*
+ 47	300,000
+ 50	200,000
LST06 = H((0)) + 51	100,000

Range list for Sun

Location	*Value, km*
H((0)) + 52	10^{9}
+ 53	600×10^{6}
+ 54	300×10^{6}
+ 55	100×10^{6}
LST02 = H((0)) + 56	40×10^{6}

It would probably be worthwhile to conduct analytic and experimental studies to redistribute the range intervals to reduce machine running time.

1. MARK locations used

HD: Flag: 0 = no uncompleted double
1 = doubling not completed

ND: If HD = 0, is 0. Otherwise number of doubles to be completed − 1.

J: Number of Runge-Kutta steps completed + 1.
$J \leq m + 1$, where m = order of the highest difference retained in the Adams-Moulton integration.

ABTB: MARK subroutine which inspects HBANK1 and HBANK2 to determine need for additional halving or doubling.

2. Contents of HBANK

HBANK2 address = number of halves
HBANK1 address = number of doubles
HBANK h_0: initial step for Runge-Kutta